Nuclear structure of ^{176}Lu and its astrophysical consequences. I. Level scheme of ^{176}Lu

N. Klay,* F. Käppeler, H. Beer, and G. Schatz
Kernforschungszentrum Karlsruhe, Institut für Kernphysik, D-7500 Karlsruhe, Germany

H. Börner, F. Hoyler,† S. J. Robinson, K. Schreckenbach, and B. Krusche‡
Institut Laue-Langevin, F-38042 Grenoble, France

U. Mayerhofer, G. Hlawatsch, H. Lindner, and T. von Egidy
Physik Department, Technische Universität München, D-8046 Garching bei München, Germany

W. Andrejtscheff and P. Petkov
Institute for Nuclear Research and Nuclear Energy, Bulgarian Academy of Sciences, 1784 Sofia, Bulgaria
(Received 27 September 1990)

Excited states of the deformed odd-odd nucleus ^{176}Lu have been investigated by the following experiments: measurement of the ^{175}Lu$(n,\gamma)^{176}$Lu reaction with high resolution crystal spectrometers and of the ^{175}Lu$(n,e^-)^{176}$Lu reaction with a double focusing magnet-spectrometer. In total, 509 gamma transitions could be identified in ^{176}Lu, and multipolarities were determined for 228 of these transitions. Additionally, a measurement of γ-γ coincidences after neutron capture and an investigation of the ^{175}Lu$(d,p)^{176}$Lu transfer reaction were also performed. Information on the lifetimes of relevant levels was obtained by the technique of delayed coincidences, and, in one case, by the Doppler shift attenuation method. With these results, a level scheme was established, comprising 97 energy levels connected by 270 gamma transitions. About 30 Nilsson configurations and corresponding rotational bands were identified. The comparison with model calculations indicates that the level scheme comprises *all* excited states with spins $1 < I < 8$ up to 900 keV. In particular, this scheme contains transitions that connect the $I^\pi = 7^-$ ground state with the 1^- isomer via mediating levels at higher excitation energy. From this coupling, the excitation energy of the isomer was precisely defined to 122.855±0.009 keV. Accordingly, the neutron separation energy of ^{176}Lu could be revised to 6287.91±0.15 keV. Based on the fact that more than 90% of the observed intensities could be placed in the level scheme, an isomeric ratio, $\sigma_p(i)/\sigma_{\text{tot}} = 0.870 \pm 0.025$, was deduced for the fractional population of the isomer by thermal neutron captures.

I. INTRODUCTION

Apart from its general importance for nuclear structure studies, ^{176}Lu is of great importance for nuclear astrophysics. While it was long considered to represent a galactic chronometer [1–3] because of its long half-life of 40.8×10^9 yr, there is increasing evidence that its half-life was strongly affected in the hot stellar photon bath through a thermal coupling between ground state and the short-lived beta unstable isomer ($t_{1/2} = 3.68$ h) [4–6]. Since direct transitions are strongly forbidden ($\Delta I = 6$, $\Delta K = 7$), this mechanism is expected to work via higher lying states of intermediate spins and K quantum numbers.

Experimentally, such electromagnetic transformations between ground state and isomer were obtained by photoactivation of Lu samples in intense gamma-ray fields [7–9]. In these measurements, the isomer could be produced only with ^{60}Co and ^{24}Na sources but not with ^{137}Cs, a hint that the mediating levels are at excitation energies above the 662 keV gamma-ray energy of ^{137}Cs. However, quantitative information on the stellar transition rates could not be inferred from these measurements as the relevant properties of the mediating levels, i.e., excitation energies and quantum numbers, remained unknown.

An improved theoretical approach was presented by Gardner *et al.*[10] who complemented the experimentally determined levels in ^{176}Lu by postulated states inferred from systematic trends in neighboring nuclei. With this "complete" level scheme it was possible to demonstrate that the temperature dependence of the ^{176}Lu half-life could be obtained without violating the K-selection rule. This result underlines the importance of an experimental extension of the level scheme, which ultimately resolves the remaining uncertainties.

Another possible mechanism for exciting ^{176}Lu is by positron annihilation with a K-shell electron [9,11]; however, the effect of this mechanism has probably been overestimated in the stellar plasma and may be important only at higher temperatures [12].

It is the aim of this work to establish the complete level scheme of ^{176}Lu, with the best experimental resolution and sensitivity, up to excitation energies of ~1 MeV, and to identify the mediating levels for isomer and ground state (paper I). On this basis, the influence of temperature on the nucleosynthesis of ^{176}Lu and its astrophysical implications are discussed (paper II).

II. THE LEVEL SCHEME

The level scheme of deformed odd-odd nuclei can be characterized by two decoupled mechanisms, intrinsic and collective excitations. The intrinsic excitations are due to single-particle excitations of the two unpaired nucleons and their residual interaction. The single particle excitations are described in the Nilsson model[13] by the quantum numbers $\Omega^{\pi}[Nn_z\Lambda]$. The projections $\Omega_{p,n}$ of the angular momenta of the unpaired proton and the unpaired neutron may couple parallel or antiparallel, $K=|\Omega_p \pm \Omega_n|$, resulting in two different values of K and different energy eigenvalues according to the residual interaction of the unpaired nucleons (Gallagher-Moszkowski splitting [14]).

The level scheme of ^{176}Lu, therefore, exhibits a number of rotational bands with energies

$$E_I=\frac{\hbar}{2\Theta}I(I+1)+E_0 \ , \tag{1}$$

where Θ is the moment of inertia. These bands are characterized by the Nilsson configurations of the unpaired nucleons as well as by the values of K and parity π. A peculiarity is to be noted for bands with $K=0$, where the energy sequence of Eq. (1) is disturbed by an energy shift between members of even and odd angular momenta (Newby shift [15]).

With these classifications the level scheme can only be approximated, since the coupling between rotation and intrinsic excitations by Coriolis interaction is not considered. It is also not always possible to characterize a rotational band by a single proton-neutron pair with well-defined Nilsson parameters due to configuration mixing (K mixing).

Level spins and parities can be determined experimentally via electromagnetic transitions following neutron capture. The reaction ^{175}Lu$(n_{\rm th},\gamma)$ leads to compound states of $I^{\pi}=3^+$ or 4^+, which decay to levels with spin 2 to 5 by $E1$ and $M1$ transitions; levels with spin 1 to 6 (or higher) can then be reached in the following steps. This means that neutron capture is not selective in populating a certain class of levels. In this respect, transfer reactions represent an important complement; for example, the ^{175}Lu(d,p) reaction adds an unpaired neutron without affecting the unpaired proton in ^{175}Lu, thus involving only levels with the unpaired proton in the ground state configuration. Correspondingly, levels with the neutron in the ground state configuration are reached in ^{177}Hf(t,α) reactions. This feature of transfer reactions allows one to distinguish between intrinsic excitations and can be very useful in establishing the level scheme.

We note that configuration assignments are—to some extent—model dependent, whereas level energies, spins, and parities are rather reliably determined by the measurements. In a few exceptional cases, model predictions were used to suggest levels that are compatible with the experimental data. This refers to several 4^+ and 5^+ levels as outlined in Secs. VII and VIII.

A. Previous results

A first comprehensive level scheme was reported by Minor *et al.* [16] who investigated the gamma rays and conversion electrons from thermal neutron captures by means of solid-state detectors and combined these data with results from a (d,p) measurement [17] and the first $(n_{\rm th},\gamma)$ study using a crystal spectrometer [18]. This scheme was extended by Balodis *et al.* [19] on the basis of improved data from high resolution $(n_{\rm th},\gamma)$ and $(n_{\rm th},e)$ measurements. These authors reported five well-established rotational bands with 31 levels, and eight additional levels, which were considered as less well established. The $I^{\pi}=7^-$, $K=7$ ground state of ^{176}Lu was explained by the parallel coupling of the unpaired proton ($\frac{7}{2}^+$, [404]) and the unpaired neutron ($\frac{7}{2}^-$, [514]). The first excited state corresponds to the antiparallel coupling of the unpaired nucleons; due to the Newby shift, the lowest state in this $K=0$ band has $I^{\pi}=1^-$. Accordingly, electromagnetic transitions to the ground state are not observed as they would require multipolarity $E6$. This means that the first excited state is an isomer that beta decays directly to ^{176}Hf.

All firmly assigned gamma transitions reported by Balodis *et al.* [19] belong to cascades feeding the isomer; only two less well established transitions were suggested to lead to the ground state. In their work, the level energies are based on the reference energy of 126.5±4 keV for the isomeric state [17]. Additional levels were postulated based on a (t,α) measurement by Dewberry *et al.* [20] including the assignment of gamma transitions measured by Balodis *et al.* [19]; furthermore, the excitation energy of the isomer could be determined to 123±2 keV. However, it was not yet possible to establish a level that could decay to both, the ground state *and* to the isomer.

The ground-state band was investigated by Coulomb excitation [21,22]. From these results, Elze *et al.* [22] suggested a 5^- band head that decays to the ground state. Since also in these studies no evidence for transitions to the isomer was found, one was still left with a level scheme that was split into two independent parts, one built on the ground state and the other on the isomer, without any transitions *between* them.

The existence of two practically independent parts of the level scheme is the consequence of the K selection rules [23]; transitions within a rotational band occur with higher probability compared to transitions between different bands, since these imply a simultaneous change in the single particle structure. The probability for an interband transition is the more reduced the greater the change of the internal wave functions (characterized by ΔK). The corresponding selection rule requires the multipolarity of the transition at least to equal ΔK. Though this rule is not stringent, K-forbidden transitions exhibit a retardation, which can be estimated by an empirical hindrance factor [24]

$$\delta=10^{-2|\Delta K-L|} \ .$$

Systematic studies confirm this rule on average, but deviations up to 4 orders of magnitude are observed [25].

In ^{176}Lu, the energetically lowest Nilsson configurations of the odd neutron and the odd proton couple to rotational bands with $K=0$ and $K=7$. The direct transition from the 1^- isomer being already hindered by the high multipolarity, transitions of lower mul-

tipolarity, which were possible between higher members of these bands, are now forbidden by the K selection rule. For example, the $E2$ transition from the 5^- member of the $K=0$ band to the ground state is $|\Delta K-L|=5$-fold forbidden, corresponding to an expected hindrance factor of 10^{-10}.

All well-established levels in the work of Balodis *et al.* [19] have $K=0$ or 1. Transitions from these levels to the $K=7$ ground state are strongly K forbidden or should have high multipolarity. Since these transitions are expected to occur with small probability, only the competing strong transitions to the $K=0$ isomer could be identified so far. Levels, which can ultimately feed the ground state *and* the isomer should have intermediate K values; such levels with $K=3$, 4, or 5 are predicted by semiempirical calculations [26] only at energies above $\sim$600 keV. Between 630 and 730 keV, four bandheads with $K^\pi=4^+$, 5^+, 3^-, and 4^- are suggested in the work of Balodis *et al.* [19]; however, no firmly established assignments could be given for the members of these bands, and all related gamma transitions lead to the isomer.

Evidence for mediating levels come from a ^{175}Lu$(t,\alpha)^{176}$Lu experiment [20], where a $K^\pi=6^-$ level at 564 keV could be established, and from a Coulomb excitation measurement [22] suggesting a $K^\pi=5^-$ bandhead at $\sim$870 keV. These levels would allow for a connection of the two partial level schemes, but the experiment of Balodis *et al.* [19] was not sensitive enough for detecting direct ground-state transitions at energies above $\sim$850 keV.

We have reinvestigated the level scheme of ^{176}Lu with the gamma spectrometers GAMS [27,28] at the high flux reactor of the Institut Laue-Langevin (ILL) Grenoble, which yield excellent resolution up to $\sim$1 MeV. Complementary information on the conversion electron spectrum for multipolarity determination was obtained with the magnetic spectrometer BILL [29] at the ILL that has an energy resolution compatible with the gamma spectra. An additional measurement of γ-γ coincidences with two germanium detectors served for the reliable assignment of the gamma transitions within the level scheme, and information on the lifetimes of relevant levels was obtained from a measurement of delayed coincidences as well as from the Doppler-broadened line shape in the gamma spectra.

The measurements in Grenoble were supplemented by the study of the ^{175}Lu$(d,p)^{176}$Lu reaction at the tandem accelerator of the Technical University Munich; the results obtained in this experiment were important for determining the energy of the $I^\pi=1^-$ isomer as well as for the assignment of levels at high excitation energies.

III. EXPERIMENTS

A. (n,γ) studies with the GAMS spectrometers

The crystal spectrometers. The bent crystal spectrometers GAMS1,2,3 are described in detail in Ref. [27]. The spectrometers are mounted at both ends of a horizontal beam line that passes the reactor core tangentially. On one side, the spectrometer GAMS1 covers the energy range $E_\gamma<400$ keV, and on the other side GAMS2,3 can be used for energies larger than $\sim$200 keV. The sample in the central position is exposed to a thermal flux of $\sim 5.5\times10^{14}$ neutrons/(s cm^2). Gamma rays from the sample are diffracted by bent quartz crystals; they are then detected by NaI scintillators in GAMS2,3 and by a Ge detector in GAMS1 [30]. Crystals and detectors are rotated in small steps by means of interferometers for defining the gamma-ray energy via Bragg's law

$$E_\gamma=\frac{nhc}{2d\sin\varphi}$$

where n is the order of reflection and $d=246$ pm the lattice constant of quartz.

The standard energy resolution of GAMS1

$$\Delta E_\gamma=\frac{E_\gamma^2 2d}{nhc}\cos\varphi\,\Delta\varphi$$

is $\sim$3 arc sec [27]. In the present measurement values of 1.8 and 2.2 arc sec above and below 100 keV could be achieved, respectively. Also for GAMS2,3 the standard resolution of $\Delta\varphi=0.8$ arc sec reported by Koch *et al.* [27] could be improved in the present measurement, where $\Delta\varphi$ was between 0.59 and 0.62 arc sec for GAMS 2 and between 0.61 and 0.64 arc sec for GAMS3. While GAMS1 is most sensitive around 150 keV, GAMS2,3 exhibits its maximal sensitivity above 450 keV, and is, hence, complementary in efficiency. Therefore, the results obtained with GAMS1 and GAMS2,3 are combined in the energy range between 150 and 400 keV, while the regions below 150 keV and above 400 keV are covered by GAMS1 or GAMS2,3, respectively.

Measurements on two lutetium isotopes. The reaction ^{175}Lu$(n,\gamma)^{176}$Lu was investigated with a 30 mg target of Lu_2O_3 enriched to 99.8% in ^{175}Lu. Due to the large difference in the thermal capture cross sections of ^{175}Lu and ^{176}Lu (23 and 2100 b), captures on the remaining 0.2% ^{176}Lu caused a significant background of gamma-ray lines from the ^{176}Lu$(n,\gamma)^{177}$Lu reaction. For the unambiguous discrimination of these ^{177}Lu lines, a second measurement was performed with a target that was enriched in ^{176}Lu (27.1%). Compared to the intensities from the ^{175}Lu$(n,\gamma)^{176}$Lu reaction, the ^{177}Lu lines should then be enhanced by a factor 190. Since the ^{176}Lu burns out rapidly in the high neutron flux, this factor decreases with time to $\sim$45 at the end of the measurement. Even in the first measurement, the burn-out of ^{176}Lu was evident by a 50% decrease of the ^{177}Lu lines. For ^{175}Lu, the smaller cross section prevents such an effect.

Normally, the ^{177}Lu background lines can be identified and be eliminated from the true spectrum of the ^{175}Lu$(n,\gamma)^{176}$Lu reaction by their intensities being time-dependent and very different in the two measurements. However, for superpositions of lines from ^{176}Lu and ^{177}Lu, the discrimination is less stringent. For example, an increase in intensity by an intermediate factor of $\sim$80 in the second measurement could indicate a ^{177}Lu line that appears weaker due to previous burnout *or* a ^{176}Lu line superimposed by a ^{177}Lu line. Such cases are included in the list of ^{176}Lu transitions but are marked as possible ^{177}Lu lines.

In addition to background lines from ^{177}Lu, the spectra contain even lines from impurities produced by double neutron captures on ^{176}Lu in the high-neutron flux. Their intensities increase with time, and they appear with higher intensities in the second measurement as well. A critical example is the 93.184 keV transition in ^{178}Hf following the beta decay of ^{178}Lu. This transition overlaps with a ^{176}Lu line as can be verified by comparison with the measurement of Maier [18], who found a line at almost the same energy but with lower intensity. Since the neutron flux was ten times smaller in that work, resulting in a 100-fold suppression of double neutron captures, the intensity reported by Maier [18] was adopted as the true ^{175}Lu(n,γ) contribution for further analysis.

Measured spectra. Figure 1 shows a small part of the gamma-ray spectrum from the ^{175}Lu$(n,\gamma)^{176}$Lu reaction measured with GAMS1 between 30 and 250 keV. Obviously, even the excellent resolution of the crystal spectrometer leaves some doublets unresolved. The best sensitivity is achieved in second order of reflection, since the reflectivities in first and second order are approximately equal but the resolution in second order is twice as good. Since the reflectivity decreases in higher orders, these spectra are less sensitive, but still useful because of their better resolution. In scanning the entire angular range of the spectrometer, many lines are measured repeatedly in different orders of reflection; their energies and intensities are determined from the mean of all results.

The same techniques for data accumulation and analysis were used for GAMS2,3. Figure 2 presents a region of particularly high line density measured in second order. Comparison of these spectra, which were taken simultaneously and independent of each other, allows for a more reliable discrimination of weak lines from random background fluctuations. Regions of high line density were measured several times and analyzed separately. At high energies, the resolution of individual lines is limited by its E_γ^2 dependence. Given the line density of the ^{176}Lu spectra, this means that the useful range of the most sensitive second order of reflection ends at $\sim$1.1 MeV, cor-

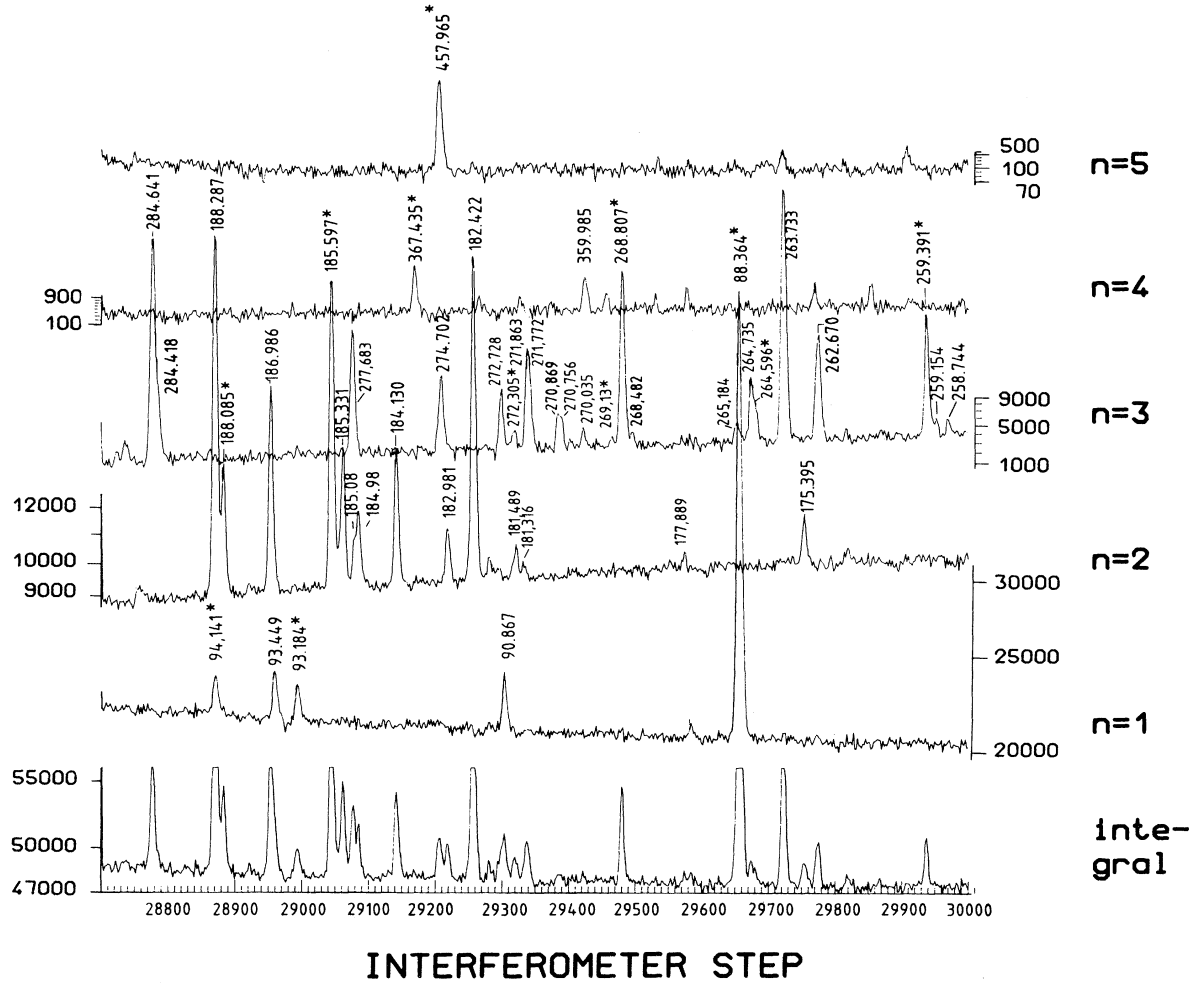

FIG. 1. Part of the spectrum measured with GAMS1 for the ^{175}Lu$(n,\gamma)^{176}$Lu reaction. The rates in the various orders of reflection (counts per 20 s) are plotted versus the interferometer steps corresponding to the angle of deflection. The gamma-ray energies are given in keV, and lines from neighboring isotopes are marked by asterisks.

responding to an energy range in first order from 150 to 550 keV.

The resolution of the GAMS2,3 spectrometers is demonstrated in Fig. 3 at the example of the multiplet at 425 keV. While the first order of reflection shows a broad complex structure, the individual components are easily resolved in third order, where the energy resolution is 70 eV.

In the energy range between 150 and 450 keV, the results obtained with GAMS1 and GAMS2,3 were combined into a common data set. The energy scale was calibrated by the $K_{\alpha 2}$ x-ray line of lutetium with the energy $E = 52.9650$ keV given by Bearden [31]. If necessary, renormalization to a different reference energy can be performed by multiplying all gamma-ray energies with a constant factor.

The experimental intensities were normalized and corrected for gamma-ray self-absorption. A first normalization to the absolute intensities of Minor [16], however, led to inconsistencies of the population balance in the well-established part of the level scheme. Therefore, the normalization was modified such that the population of isomer and ground state together did not exceed 100%. The absorption corrections below 200 keV were chosen to be consistent with the population balance, i.e., that levels are not more strongly populated than depopulated. A list of all gamma transitions is given in Table I.

B. Measurement of the conversion electron spectrum with BILL

Electron spectrometer. A detailed description of the double focusing magnetic spectrometer BILL is to be

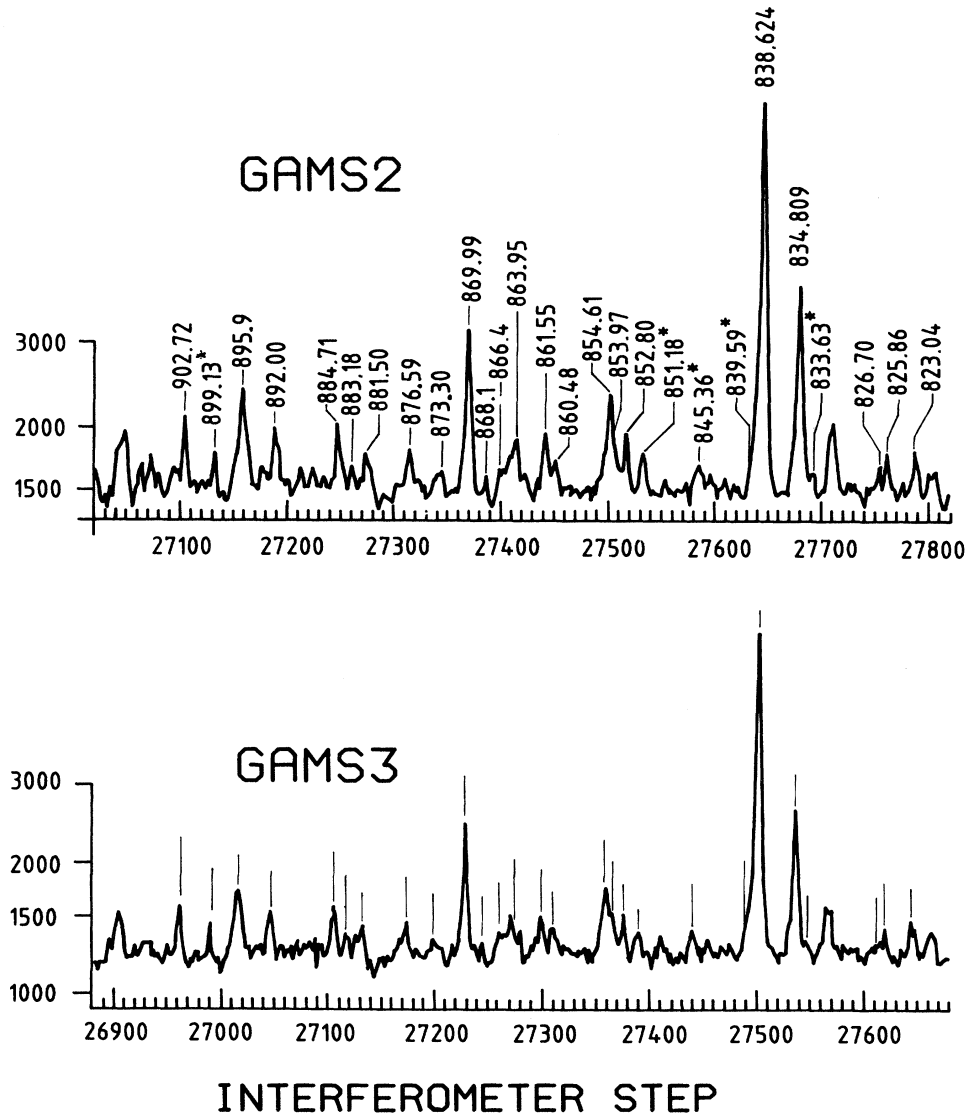

FIG. 2. The spectrum in a region of high line density measured with the spectrometers GAMS2,3 in second order of reflection (counts per 20 s).

found in Ref. [29]. The spectrometer is installed at the end of a 14-m-long, vertical beam line at the upper level of the reactor; it consists of two independent flat electromagnets, which act as double focusing spectrometers. The sample with a maximum size of 40 cm^2 is located in a neutron flux of $\sim 3.0\times 10^{14}$ neutrons/($s\,cm^2$). The first magnet with a deflecting angle of 58° produces a small intermediate image that is viewed by the second, high dispersion magnet, which has a deflection angle of 270°. The electrons are finally recorded by a position sensitive 32-wire proportional counter in the extended focal plane of the spectrometer. The electron momentum can then be derived by the combined information on position and magnetic field. The magnetic field was changed in well-defined steps such that an electron with given momentum p is detected by subsequent wires. The measured spectra are recorded for all wires individually and are added later onto a common sum spectrum by due consideration of the momentum shift between the wires. In this way, each point in the sum spectrum corresponds to the sum of 32 single measurements at different times. The momentum resolution in standard experiments is

$$\frac{\Delta p}{p}=4\times 10^{-4}\ ,$$

if sufficiently thin targets are used.

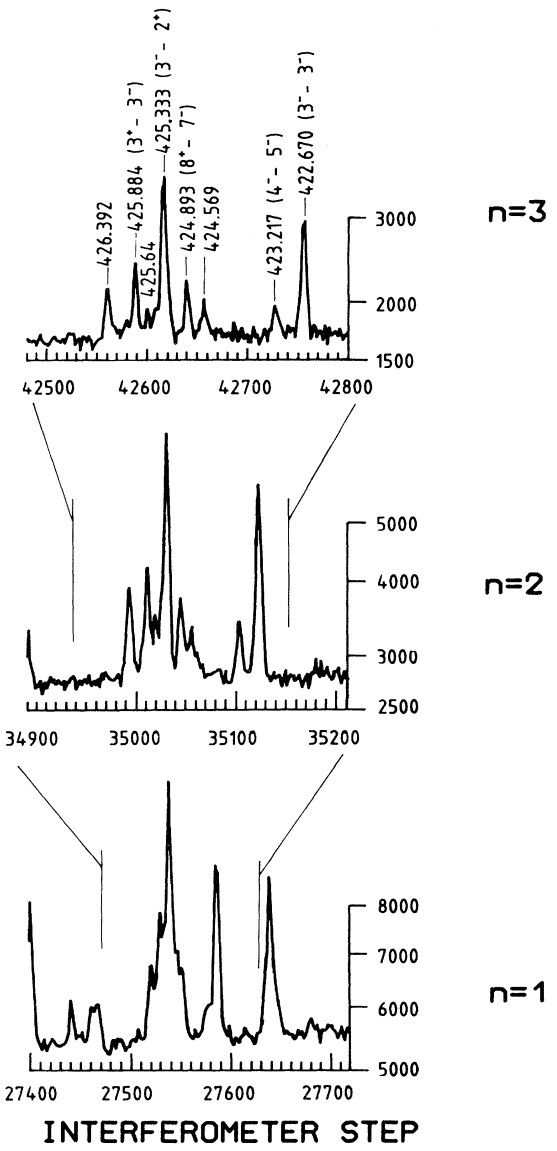

FIG. 3. An example for the improved energy resolution in the spectra of higher order. The multiplet at 425 keV can be completely resolved in third order. The numbers in brackets behind the gamma-ray energies denote the assignment of these transitions in the level scheme.

Samples for the (n,e^-) *reaction.* The sample thickness is necessarily a compromise between resolution and sensitivity. In order to maintain good conditions over the entire energy range, the measurements were carried out with two targets: for electron energies below 250 keV, the target thickness was limited to $\sim 80\ \mu g/cm^2$, while a $\sim 250\ \mu g/cm^2$ thick target could be used at higher energies without a noticeable loss in resolution.

The targets were prepared from a 2g pellet of Lu_2O_3 enriched in ^{175}Lu to 99.8%. This pellet was evaporated by an electron gun onto aluminum foils 14×4 cm^2 in size and 0.2 and 1 mg/cm^2 thick for the thin and thick Lu_2O_3 samples, respectively. In order to avoid contamination from the copper boat, the enriched pellet was lined underneath with a second pellet of natural Lu_2O_3. Homogeneity and thickness of the 10×3 cm^2 large evaporated layers were measured by Rutherford backscattering with 2 MeV protons[32]. The samples were found to be homogeneous within ±6%. The final enrichment was somewhat less than 99.8% ^{175}Lu, since a minor part of the natural lutetium pellet (97.4% ^{175}Lu) was evaporated as well.

Measurements and results. With the thin target, the energy range between 16 and 250 keV was covered in momentum steps $\Delta p/p=1.37\times 10^{-4}$. A section of that spectrum is shown in Fig. 4. At low energies, the line density in the electron spectrum is significantly higher compared to the gamma spectrum, since there are *K-, L-, and M*-conversion lines from all but the weaker gamma transitions. The three lines from the L subshells can be well separated for individual transitions. However, superpositions of lines from different transitions and subshells cannot always so unambiguously be distinguished as for the example of the K and L_2 lines in Fig. 4.

At lower energies, the line shape becomes increasingly asymmetric due to energy losses in the sample. This effect can be well described by an asymmetric Gaussian shape superimposed with an exponential on the low energy side [27,33]. In the second experimental run with the 250 $\mu g/cm^2$ sample, the energy range from 100 to 760 keV was covered twice. The region between 760 and 840 keV was scanned 5 times in order to achieve higher sensitivity. The resulting spectrum of Fig. 5 shows that good energy resolution could be maintained during this multiscan procedure. Energy calibrations were performed for each run separately by means of the known gamma tran-

TABLE I. Energies, intensities, and multipolarities of the measured gamma transitions in ^{176}Lu. For the gamma energy, absolute uncertainties are given (in keV), whereas relative uncertainties (in %) are quoted for the intensities. The following abbreviations are used in columns 4 and 8. 1: gamma transitions strongly affected by a line from a neighboring isotope, normally from ^{177}Lu; *Z*: doubtful line, close to the sensitivity limit and statistically not significant; *D*: transition belonging to an unresolved doublet with relatively large uncertainties. Assigned transitions are marked by a (+) in front of the energy value. *M*: Gamma data from Ref. [18].

Gamma-ray energy (keV)	Intensity per 100 n	Multipolarity	Comment
1130.372 0.095	0.37 12		
1120.053 0.111	0.21 15		
1093.980 0.127	0.20 15		1
1091.935 0.103	0.23 13		
1055.597 0.099	0.21 14		
1052.155 0.067	0.34 25		
1048.832 0.064	0.24 20		1
1043.132 0.154	0.13 16		
1042.140 0.054	0.23 21		
1038.688 0.095	0.59 10		1
1035.181 0.029	0.37 12		
+1032.365 0.043	0.24 11		
1028.604 0.109	0.13 16		
1026.443 0.064	0.16 12		1
1022.307 0.078	0.14 12		1
1019.185 0.081	0.21 11		
1009.641 0.100	0.23 12		1
1005.600 0.039	0.23 12		
+1002.494 0.273	0.07 21		1
+1000.753 0.073	0.13 14		1
999.492 0.099	0.15 15		1
995.159 0.092	0.12 17		
991.810 0.054	0.14 12		
988.526 0.087	0.13 17		
986.608 0.082	0.20 12		
980.329 0.197	0.08 17		1
977.245 0.061	0.24 13		
975.801 0.022	0.38 13		
+972.481 0.035	0.22 20		
961.971 0.091	0.09 16		
957.822 0.042	0.15 29		1
954.688 0.038	0.15 17		1
+938.365 0.057	0.09 19		
931.195 0.065	0.11 21		1
928.351 0.101	0.09 34		1
926.681 0.031	0.24 17		
925.171 0.047	0.11 13		1
+921.464 0.013	0.62 10		
915.588 0.056	0.18 24		
913.700 0.074	0.09 26		
909.976 0.054	0.28 16		
+906.783 0.047	0.13 27		1
903.713 0.070	0.22 12		1
902.718 0.021	0.26 10		
896.068 0.035	0.35 38		*D*
895.403 0.160	0.15 25		1 *D*
893.304 0.098	0.09 19		1
892.000 0.025	0.21 11		1
884.712 0.018	0.23 12		
883.183 0.050	0.10 24		
881.500 0.023	0.17 12		
873.299 0.041	0.11 12		1
+869.994 0.011	0.84 10	*E*2	
+868.126 0.117	0.07 16		1
866.374 0.099	0.05 25		
863.954 0.047	0.10 25		1
861.554 0.021	0.18 10		
860.477 0.042	0.09 12		
855.212 0.065	0.09 17		1
+854.614 0.023	0.33 10	*E*1	
853.970 0.035	0.15 12		
852.797 0.016	0.19 13		
848.555 0.102	0.13 16	(*M*1,*E*2)	
841.902 0.118	0.11 17		
+838.624 0.007	3.41 10	*E*2	
+834.810 0.007	0.91 10	*E*2	
826.702 0.084	0.08 13	*M*1	
825.860 0.026	0.13 18	*M*1	
821.253 0.068	0.11 28		1
+818.914 0.109	0.10 17	(*M*1)	
+816.719 0.018	0.31 12	(*E*2,*M*1)	
814.449 0.038	0.10 20		1
812.324 0.065	0.20 12		1
796.404 0.045	0.10 14		
794.499 0.041	0.08 40		
+792.746 0.054	0.10 15		1
787.420 0.019	0.24 15		1
+786.808 0.135	0.10 30		
777.568 0.034	0.09 13		
+765.684 0.009	0.52 10	*M*1	
747.937 0.012	0.30 11	(*M*1,*E*2)	
743.788 0.052	0.10 16		
739.918 0.026	0.11 14		
+736.422 0.021	0.18 30	(*E*2)	
735.404 0.034	0.12 35		
732.461 0.076	0.10 16		
730.936 0.040	0.43 21		
730.581 0.071	0.14 21		
+730.264 0.040	0.12 13		
+727.094 0.013	0.40 16	(*E*1,*E*2)	
+724.636 0.053	0.13 13	(*E*1,*E*2)	
+721.968 0.007	0.72 10	*M*1	
719.571 0.053	0.13 13		1
712.817 0.021	0.15 16		1
+709.555 0.006	0.74 11	*M*1(+*E*2)	*D*
+709.230 0.012	0.27 16	(*E*2,*E*1)	*D*
705.743 0.033	0.15 12	(*M*1)	
704.299 0.063	0.09 16	(*M*1,*E*2)	
+697.614 0.042	0.12 31	(*M*1)	
696.023 0.025	0.20 15	(*M*1,*E*2)	
692.295 0.022	0.22 16	(*M*1,*E*2)	*D*
691.872 0.016	0.28 14	(*M*1,*E*2)	*D*
691.056 0.018	0.18 21	(*M*1)	
688.635 0.010	0.31 21	(*M*1,*E*2)	
683.205 0.041	0.09 14		
680.961 0.040	0.10 14		

TABLE I. (*Continued*).

Gamma-ray energy (keV)		Intensity per 100 n		Multipolarity	Comment
675.793	0.054	0.18	21	(*M*1)	
675.114	0.037	0.17	28	(*M*1)	
+673.878	0.064	0.16	26		
+672.655	0.101	0.07	17		
+671.992	0.007	0.48	11	*M*1(+*E*2)	
670.012	0.039	0.10	35	(*M*1,*E*2)	
+669.327	0.132	0.05	21		
+667.356	0.021	0.33	10	*M*1(+*E*2)	
+660.801	0.028	0.29	12		
+658.384	0.042	0.11	13		
+657.334	0.023	0.16	11	(*M*1,*E*2)	
653.477	0.031	0.10	13		
+652.574	0.036	0.09	14		1
651.492	0.080	0.05	21		
650.652	0.041	0.08	15		
646.174	0.028	0.12	18		
+643.115	0.010	0.28	13	*M*1(+*E*2)	*D*
+642.890	0.014	0.20	15	(*E*2)	*D*
641.660	0.028	0.13	32		
639.836	0.020	0.07	66		1
637.015	0.032	0.13	12		
636.281	0.023	0.11	17		
+633.249	0.008	0.53	11	*M*1+*E*2	
+631.396	0.013	0.31	10	*M*1	
627.544	0.008	0.21	10	(*M*1,*E*2)	
+624.834	0.022	0.32	11	*M*1	
617.894	0.025	0.11	13	(*M*1)	
604.145	0.020	0.10	29	(*M*1)	
599.488	0.024	0.13	12	(*M*1,*E*2)	
+597.879	0.028	0.11	12		
+596.627	0.006	0.40	12	*M*1	
+595.569	0.039	0.08	14		
594.341	0.032	0.09	13		*Z*
587.581	0.023	0.15	11		
586.086	0.029	0.13	12	(*M*1)	
582.646	0.037	0.08	14		
+581.608	0.046	0.08	21		
+578.743	0.017	0.25	13	*M*1	
+578.198	0.008	0.75	10	*M*1	
+573.563	0.026	0.08	13		
567.832	0.035	0.09	13	(*M*1)	
+566.990	0.015	0.41	12	(*M*1,*E*2)	
+565.241	0.009	0.28	11	*M*1	
+563.944	0.003	2.39	10	*M*1(+*E*2)	
+562.556	0.033	0.09	12	(*M*1)	
+561.253	0.034	0.08	16		
+559.714	0.015	0.17	12	*M*1	
+559.157	0.033	0.09	13		
+558.237	0.019	0.21	11	(*M*1,*E*2)	
556.329	0.038	0.08	13		
+549.389	0.011	0.54	11	*M*1	
544.540	0.026	0.14	19		1
539.691	0.025	0.07	14		
528.648	0.035	0.12	16		
+527.501	0.008	1.00	13	*M*1	
+527.174	0.020	0.17	15	*M*1	
+524.817	0.013	0.16	11	*M*1	
+520.404	0.037	0.15	12	(*M*1)	
514.702	0.034	0.09	16		1
499.458	0.016	0.10	11		1
+497.898	0.011	0.06	15		1
497.568	0.012	0.06	15		
495.439	0.026	0.03	22		
493.710	0.006	0.21	10	*M*1	
492.591	0.069	0.04	16		
+491.365	0.008	0.17	12	*M*1	
490.296	0.239	0.02	23		1
+487.819	0.023	0.07	15		
+487.149	0.027	0.05	13		
+485.006	0.006	0.11	10	*M*1	
+480.661	0.013	0.08	11	(*M*1)	
+479.756	0.006	0.12	11		
478.161	0.011	0.07	12	(*M*1)	
477.207	0.011	0.07	12	(*M*1,*E*2)	
+473.276	0.043	0.03	24		1
472.460	0.074	0.02	40		
+471.652	0.016	0.04	16		
470.410	0.017	0.05	17		
470.169	0.026	0.03	23		
+468.500	0.012	0.04	25		
467.372	0.024	0.05	20		
+466.107	0.017	0.02	24		
465.026	0.065	0.02	21		
464.007	0.018	0.08	21		
463.396	0.022	0.04	22		
461.671	0.012	0.05	16		
460.967	0.010	0.10	11	(*E*2)	
459.748	0.025	0.03	28		1
459.094	0.019	0.05	17		
457.425	0.015	0.10	21		1
453.471	0.034	0.04	14		
+452.990	0.011	0.08	13	(*M*1)	
+452.105	0.008	0.07	12		
449.853	0.011	0.09	14		
447.578	0.011	0.09	12	(*M*1)	
447.111	0.070	0.03	24		
446.074	0.009	0.10	11		1
444.532	0.009	0.06	13		
443.486	0.023	0.06	14		
440.397	0.017	0.08	12	(*M*1)	
439.630	0.003	0.23	10	*M*1	
439.035	0.035	0.03	21		
+437.479	0.043	0.04	18		
+435.068	0.027	0.06	26		
+433.325	0.003	0.32	12	*E*1	
432.773	0.034	0.03	21		
430.928	0.008	0.08	13		1
430.273	0.030	0.03	22		1
+429.772	0.005	0.07	13	(*M*1)	
429.368	0.005	0.09	17	(*M*1)	
426.392	0.004	0.16	10		1
+425.884	0.003	0.21	11		

TABLE I. (*Continued*).

Gamma-ray energy (keV)	Intensity per 100 n	Multipolarity	Comment
425.640 0.008	0.10 11		1
+425.333 0.002	0.60 10	(*E*1,*E*2)	
+424.893 0.004	0.14 13	(*E*2,*E*1)	
424.569 0.008	0.09 12	(*M*1)	
+423.217 0.004	0.09 15	(*M*1)	
+422.670 0.002	0.39 10	*M*1	
421.712 0.036	0.03 31		
+421.014 0.069	0.03 18		1
+419.701 0.003	0.34 10	*M*1	
419.306 0.018	0.09 27		
417.346 0.029	0.04 15		
416.184 0.018	0.05 16		
412.727 0.033	0.03 28		1
+410.892 0.005	0.12 11	*M*1	
+410.381 0.005	0.12 10	*M*1	
+408.946 0.012	0.06 16		
405.532 0.030	0.05 12		
403.758 0.012	0.06 16		
402.816 0.002	0.26 10	(*M*1)	
+402.109 0.015	0.04 18		1
+399.555 0.087	0.02 28		1
+398.942 0.018	0.04 16		
+397.653 0.013	0.04 19		1
395.801 0.034	0.04 17		
395.165 0.024	0.05 13		
394.141 0.008	0.08 19	*M*1	
392.635 0.010	0.16 12	*M*1	
+392.413 0.005	0.30 10	*M*1	
+391.909 0.022	0.06 16		1
390.754 0.022	0.06 16		1
+388.901 0.019	0.06 12	(*E*2)	
388.044 0.013	0.07 12		
+384.726 0.009	0.08 13	(*M*1,*E*2)	
383.461 0.019	0.07 12	(*M*1,*E*2)	
+382.030 0.006	0.13 11	(*M*1,*E*2)	
+381.156 0.029	0.05 13	(*M*1?)	
377.017 0.009	0.07 11	(*M*1)	
375.936 0.016	0.08 13		
368.540 0.011	0.11 11	(*M*1)	
366.185 0.016	0.06 16	(*E*2)	
364.303 0.015	0.09 12		
+362.789 0.004	0.26 11	(*M*1,*E*2)	
361.800 0.010	0.06 12		
+361.485 0.005	0.13 10		
+359.985 0.004	0.82 10	*M*1+*E*2	
+359.083 0.003	0.28 10	(*E*1,*E*2)	
+357.539 0.010	0.07 12	(*M*1)	
+355.682 0.002	0.41 10	*M*1+*E*2	
+353.158 0.007	0.06 12	(*M*1)	
+350.364 0.002	0.42 10	*M*1	
+346.618 0.005	0.16 10	(*M*1)	
+346.093 0.011	0.06 16	(*M*1)	
+344.493 0.007	0.08 11	(*M*1)	
+342.923 0.011	0.07 13		
+342.163 0.036	0.04 20		
+338.556 0.003	0.43 10	*M*1	
337.456 0.008	0.08 12		
+335.851 0.001	4.65 10	*M*1+*E*2	
+335.007 0.006	0.11 11		
+332.462 0.012	0.05 13	(*M*1,*E*2)	
+330.597 0.002	0.64 10	*M*1(+*E*2)	
328.945 0.007	0.10 13	*E*2	
+328.432 0.005	0.14 10	*M*1	
+327.099 0.012	0.05 15		
325.086 0.007	0.10 12		
321.726 0.010	0.08 16		
320.636 0.005	0.17 10	(*M*1)	
317.476 0.020	0.04 20		1
+317.099 0.016	0.05 17		
+316.630 0.006	0.10 11		
315.585 0.009	0.06 13		
312.365 0.039	0.04 22		
311.251 0.018	0.06 13		
310.890 0.003	0.39 10	*M*1	
310.785 0.018	0.13 42		1
+310.188 0.002	5.36 10	*M*1	
+309.421 0.008	0.09 12		
+309.142 0.003	0.29 10	(*M*1)	
+306.069 0.006	0.06 12	(*M*1,*E*2)	
+303.793 0.006	0.04 18		1
+303.058 0.039	0.04 22	(*M*1,*E*3)	
+301.749 0.002	0.15 10	*M*1	
+301.284 0.002	0.49 11	*M*1	
299.888 0.004	0.09 13	*M*1	
+299.449 0.001	0.39 11	*M*1	
299.147 0.016	0.04 21	(*M*1)	
+296.397 0.005	0.07 12	(*M*1,*E*2)	
292.537 0.003	0.15 10	*M*1	
292.000 0.039	0.03 24	(*M*1,*E*2)	*Z*
+287.364 0.004	0.10 11	*M*1,*E*2	
+286.555 0.049	0.02 39		*Z*
+285.948 0.006	0.04 15		
285.685 0.004	0.11 42	*M*1	
+285.571 0.004	0.11 11		
+284.641 0.001	2.94 10	*M*1	
+284.418 0.003	0.28 10	*M*1	
+277.683 0.001	0.88 10	*M*1	
276.425 0.030	0.03 28	(*M*1)	*Z*
+274.702 0.002	0.44 10	*M*1	
+272.729 0.003	0.33 10	*M*1	
+271.863 0.004	0.57 10	(*E*2)	*D*
+271.772 0.006	0.25 13		*D*
+270.869 0.003	0.13 11	*M*1	
+270.756 0.004	0.11 12		
270.454 0.019	0.03 28		1
+270.035 0.005	0.07 13	(*M*1)	
+269.125 0.013	0.04 20	(*M*1)	
268.482 0.005	0.08 12		
265.184 0.006	0.09 11	*M*1	
265.008 0.020	0.05 21		*Z*
264.735 0.003	0.32 10	*M*1	
+263.733 0.002	3.48 10	*M*1+45(10)%*E*2	

TABLE I. (*Continued*).

Gamma-ray energy (keV)	Intensity per 100 n	Multipolarity	Comment
262.670 0.003	0.77 10	$M1+E2$	
+259.154 0.011	0.08 13	$(M1,E2)$	1
+258.744 0.008	0.07 12	$M1$	
+258.511 0.045	0.03 24		Z
257.369 0.023	0.03 24		Z
256.638 0.016	0.04 18		1
256.295 0.013	0.03 62		1
+254.824 0.004	0.15 10	$M1$	
+253.858 0.007	0.10 12	$E2$	
253.356 0.047	0.03 20	$(E2)$	Z
+252.524 0.017	0.06 26		
252.256 0.003	0.22 10	$M1$	1
+251.195 0.002	0.72 10	$M1$	
+247.660 0.005	0.08 11	$M1$	
+246.994 0.012	0.05 34		
+246.305 0.005	0.09 11		
245.290 0.015	0.05 21	$(E2)$	
+244.219 0.018	0.03 37		
243.742 0.041	0.01 53		1 Z
+242.929 0.025	0.02 32		1 Z
242.362 0.005	0.09 19		
+240.760 0.002	0.32 10	$(E1,E2)$	
+239.958 0.029	0.05 47	$(E2,E1)$	
+239.910 0.052	0.02 46		
+239.383 0.011	0.05 13		1
+238.671 0.001	0.86 10	$E1$	
+236.075 0.002	0.27 11	$M1,E2$	
+234.977 0.004	0.08 12	$(M1)$	
234.752 0.003	0.10 11	$M1$	
+233.741 0.001	1.64 10	$M1$	
+228.544 0.018	0.03 19		
+227.997 0.001	2.25 10	$M1+8(3)\%E2$	
+225.403 0.001	7.02 10	$M1+7(4)\%E2$	
+222.106 0.002	0.52 10	$M1$	
+221.386 0.004	0.12 11	$M1$	
+219.282 0.002	1.01 10	$E2$	
+218.040 0.003	0.16 10		
217.922 0.012	0.03 30		
+217.002 0.001	1.42 10	$M1$	
+216.015 0.009	0.06 15		
+214.349 0.003	0.55 10	$E1$	
+214.132 0.001	0.86 10	$M1$	
212.529 0.004	0.10 16	$M1$	
+210.550 0.003	0.10 11	$E2$	
208.928 0.007	0.04 16		
+206.994 0.013	0.06 19		Z
+205.531 0.006	0.07 13		
+204.746 0.003	0.15 11	$M1$	
+203.413 0.002	0.22 10		
+201.742 0.005	0.10 11	$M1$	
+201.567 0.001	2.80 10	$E2$	
+199.926 0.001	0.21 10		
199.424 0.010	0.10 13		1
199.037 0.005	0.12 21	$E2$	
+197.547 0.010	0.04 24	$(M1)$	
+197.265 0.001	0.88 10	$M1$	
+196.400 0.011	0.03 26		1
+194.656 0.012	0.03 28		1
+194.258 0.006	0.04 34	$M1$	
+192.212 0.001	7.07 10	$E1$	
190.057 0.018	0.06 15		1
189.963 0.016	0.03 19		Z
+188.287 0.001	1.92 10	$E2$	
188.240 0.003	0.20 13		
+186.986 0.001	0.81 10	$M1$	
186.897 0.008	0.08 16		Z
+185.331 0.001	0.51 10	$M1+20(15)\%E2$	
+185.080 0.003	0.12 20	$(M1)$	
+184.980 0.002	0.28 10	$M1$	
+184.130 0.001	0.46 10	$M1+57(9)\%E2$	
+182.981 0.002	0.18 10	$M1$	
+182.422 0.001	1.68 10	$M1$	
182.073 0.006	0.04 26		
181.960 0.020	0.02 28		
181.862 0.013	0.03 23		
+181.489 0.004	0.12 12	$(E1,E2)$	
+181.316 0.006	0.06 21	$(E2)$	
177.889 0.007	0.04 28		
+175.395 0.002	0.15 10	$M1$	
175.057 0.012	0.03 20		Z
174.867 0.011	0.04 18		
172.785 0.015	0.07 21		
+171.976 0.002	0.17 10		
171.230 0.019	0.02 35		1
+169.671 0.002	0.29 10	$M1$	
+169.574 0.005	0.08 36		
+169.500 0.004	0.10 12	$(M1,E2)$	
+167.876 0.004	0.16 11	$(M1)$	1
166.973 0.016	0.03 31		Z
+166.671 0.021	0.02 45		Z
+164.120 0.007	0.04 27		
+162.713 0.004	0.08 11		
+161.277 0.004	0.06 16	$(M1)$	
+160.589 0.002	0.09 11	$(M1,E2)$	
+158.496 0.005	0.06 23		
+158.403 0.006	0.04 37		1
+156.362 0.003	0.11 14	$(E2,M1)$	
+153.557 0.002	0.27 10	$M1$	
+153.466 0.001	2.69 10	$E1$	
152.295 0.029	0.04 27		Z
+150.815 0.004	0.10 16		
+150.763 0.002	0.17 12	$M1$	
+148.676 0.010	0.04 26		
+148.241 0.001	0.23 11	$M1$	
+147.553 0.002	0.76 12	$M1$	
+147.518 0.003	0.22 29		
+145.170 0.007	0.05 23		
+145.117 0.007	0.05 23		1
+144.486 0.002	0.47 11	$M1+11(4)\%E2$	
+142.146 0.009	0.05 46		1
141.983 0.006	0.03 22		
140.497 0.002	0.14 12		

TABLE I. (*Continued*).

Gamma-ray energy (keV)	Intensity per 100 n	Multipolarity	Comment
+139.383 0.001	1.64 12	$E2$	
+137.712 0.006	0.04 29		
137.215 0.020	0.04 33		Z
+136.887 0.007	0.04 21		
136.742 0.010	0.04 19		1
+134.679 0.019	0.05 25		Z
133.937 0.009	0.03 34		Z
+133.683 0.002	0.35 10	$E1$	
+133.252 0.009	0.03 23		
+132.815 0.002	0.10 13		1
+132.364 0.009	0.04 41		
+131.987 0.030	0.04 36		Z
130.322 0.007	0.03 31		
+129.773 0.001	0.82 10	$M1$	
127.065 0.009	0.03 33		1
125.550 0.007	0.07 39	$(E2)$	
+125.350 0.017	0.05 21		Z
124.062 0.001	0.32 11	$M1$	
+120.499 0.001	0.32 10	$M1(+E2)$	
+119.678 0.001	0.39 11	$M1$	
118.725 0.002	0.21 10	$(E2)$	
+118.295 0.006	0.04 23	$(E2)$	
+118.190 0.021	0.01 82		Z
+116.763 0.004	0.06 20	$(M1)$	Z
+116.206 0.001	0.18 11	$M1$	
+115.722 0.003	0.09 15	$(M1)$	
+115.144 0.002	0.62 11	$M1(+E2)$	
+114.593 0.008	0.04 27		1
+114.070 0.002	0.11 12	$M1$	
113.945 0.012	0.07 25		Z
+112.922 0.001	5.85 16	$E2$	
112.157 0.008	0.03 38		Z

Gamma-ray energy (keV)	Intensity per 100 n	Multipolarity	Comment
111.860 0.003	0.06 16	$(M1,E2)$	
+109.541 0.006	0.05 20	$M1$	
109.398 0.006	0.06 21		Z
+105.738 0.002	0.17 17	$M1$	
+104.985 0.002	0.43 11	$E2$	
+99.163 0.001	0.57 12	$M1+3.3(15)\%E2$	
93.748 0.009	0.09 19		Z
+93.449 0.001	0.38 11	$M1$	
93.193 0.009	0.19 51	$(M1,E2)$	M
91.665 0.004	0.06 24		1
91.018 0.009	0.09 28		Z
+90.867 0.001	0.57 10	$M1(+E2)$	
90.614 0.008	0.08 22		Z
89.619 0.012	0.07 27		Z
88.862 0.003	0.14 15		1
+81.996 0.004	0.08 28		Z
+81.301 0.004	0.06 33	$M1$	
+77.623 0.004	0.10 25		Z
+73.140 0.001	1.05 10	$M1+2.5(10)\%E2$	
+71.840 0.001	0.69 15	$M1$	
+71.516 0.001	26.0 10	$E1+0.22(2)\%M2$	
+69.498 0.002	0.18 24	$(M1)$	
+66.238 0.001	1.84 12	$M1+1.7(5)\%E2$	
+65.353 0.005	0.11 35	$(M1+E2)$	Z
+64.970 0.004	0.13 31	$M1$	
+64.474 0.001	0.34 13	$M1+2.3(5)\%E2$	
+64.369 0.006	0.09 44	$(M1+E2)$	Z
+58.597 0.001	0.14 17	$M1(+E2)$	
+51.896 0.001	0.19 17	$M1+1.8(3)\%E2$	
+46.458 0.001	1.69 26	$M1+0.55(15)\%E2$	
+38.745 0.001	2.47 27	$M1+1.6(1)\%E2$	

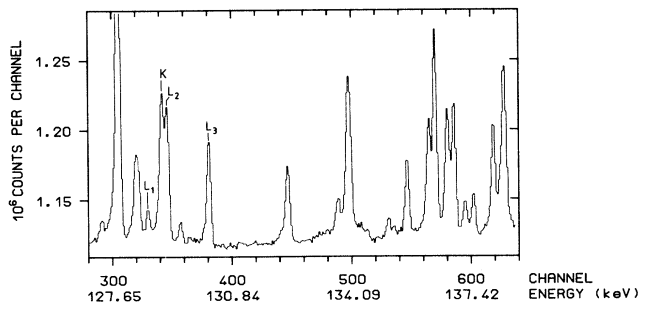

FIG. 4. Part of the conversion electron spectrum taken with the 80 $\mu g/cm^2$ sample (counts per 20 s). The indicated L lines are due to the $E2$ transition with $E_\gamma = 139.383$ keV, whereas the K line belongs to an $E1$ transition with 192.212 keV. The K and L_2 lines are separated by 140 eV.

sitions and electron binding energies.

The best momentum resolution

$$\frac{\Delta p}{p} = 3.8 \times 10^{-4}$$

was obtained in the high energy region; at lower energies, the resolution was increasingly affected by absorption losses in the sample, so that the results obtained with the thicker sample could be considered only above 170 keV.

C. Combination of (n,γ) and (n,e^-) measurements

The results for the gamma-ray energies and intensities of the observed gamma transitions in ^{176}Lu are summarized in Table I together with the multipolarities derived from the conversion electron spectra. A more detailed

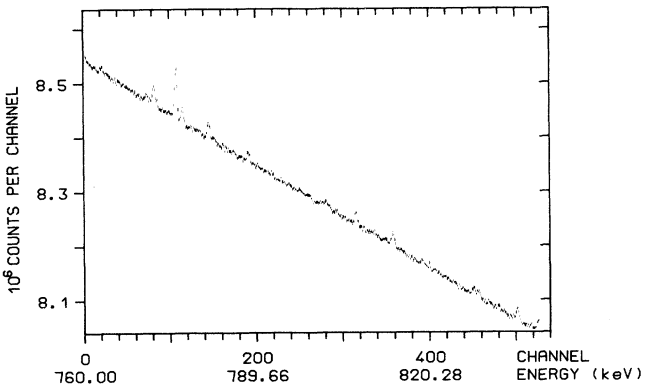

FIG. 5. The conversion electron spectrum at high energies (counts per 125 s).

table including electron energies and intensities as well as the experimental and theoretical conversion coefficients is given in Ref. [34]. Transitions that could be assigned in the level scheme are marked by a (+) in front of the energy in column 1. The intensities are quoted in number of transitions per 100 captures, and are normalized such that the population of isomer and ground state accounts for ~100%. Since not all transitions to either one of these states are necessarily assigned in the level scheme, this normalization may slightly overestimate the true intensities. On the other hand, our I_γ values are already smaller than those given in Ref. [16]. The uncertainties in I_γ are determined by the statistical uncertainty and by a constant systematic uncertainty of 10% that were added in quadrature.

The intensities of electron lines were normalized with respect to the gamma intensities such that known multipolarities were correctly reproduced. To this end, theoretical conversion coefficients were calculated with the code CATAR [35]. Multipolarities were determined by comparison of the experimental conversion coefficients

$$\alpha = I_e / I_\gamma$$

with the calculated values. Reliable multipolarities could be assigned to those transitions for which electrons from different subshells could be detected. In cases where transitions are superimposed by background lines from ^{177}Lu, conversion electron intensities may be systematically too high, since the enrichment of the sample was smaller in the electron measurements. If for such transitions only conversion electrons from the K shell were available, multipolarities could not be determined.

The abbreviations in the last column are explained in the caption of Table I; a more detailed table with energies and intensities of background lines from neighboring isotopes may be found in Ref. [34].

D. The (γ-γ) coincidence measurement

This measurement was carried out at the end of the H22 thermal neutron guide at the ILL high flux reactor. Though the flux at this position is limited to ~10^8 neutrons/(sec cm^2), there is the advantage of a large solid angle between sample and detector and of a low gamma-ray background. A sample of ~100 mg Lu_2O_3 (99.94% ^{175}Lu) inside the neutron guide was viewed by two Ge detectors at a 15 cm distance.

In establishing the level scheme, gamma-ray cascades consisting of a high energy and a low energy transition are particularly useful. Accordingly, two different detectors were used: a planar Ge detector for the energy range below 100 keV, and a larger Ge(Li) detector with good efficiency at higher energies, but with a lower limit of ~70 keV. The total measuring time was 50 hr at a coincidence rate of 400 to 450 s^{-1}. For each coincidence, the two gamma-ray signals were stored together with their time difference. From these data it was later possible to generate the coincidence spectra by means of appropriate digital energy windows. Such a coincidence spectrum is shown in Fig. 6 for the 225.403 keV line after subtraction of background from accidental coincidences and Compton scattered gamma rays. The window was set in the Ge(Li) detector, and energies are given for a number of lines.

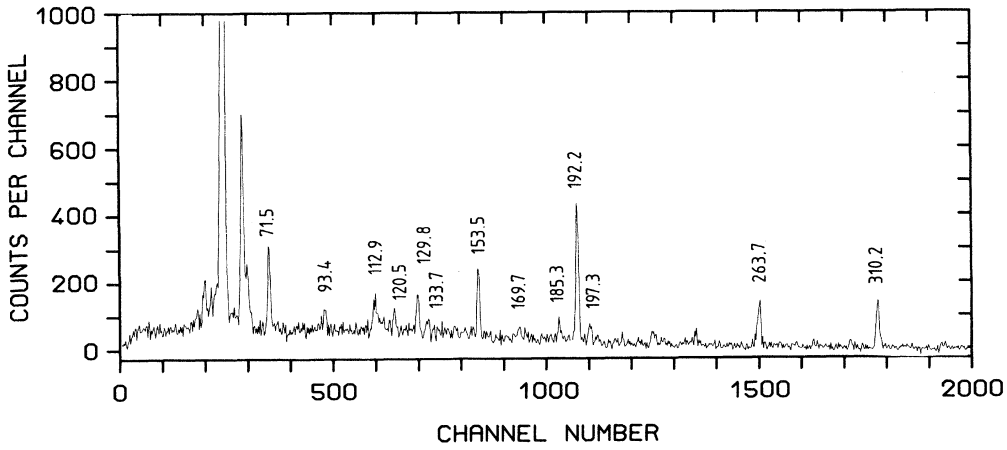

FIG. 6. Coincidence spectrum for the 225.403 keV transition. Energies are indicated for some of the transitions.

TABLE II. Results of the (γ-γ) experiment measured with the planar detector [energy windows in the Ge(Li) detector]. Classification of coincidences: S, very strong; Y, intermediate, but well established; W, weak; VW, very weak or doubtful.

	Energy window on high energy lines																
Coincident lines	214.1	219.2	222.1	225.4	227.9	233.7	240.7	251.2	262.6 263.7	277.6	284.6	299	301	310.1	335.8	422.6 425.3 425.8	563.9 565.2
38.7	. . .	. . .	. . .	. . .	. . .	. . .	. . .	. . .	. . .	. . .	. . .	. . .	. . .	. . .	VW	VW	. . .
46.5	. . .	. . .	. . .	W	. . .	. . .	. . .	. . .	VW	. . .	. . .	. . .	. . .	. . .	. . .	VW	. . .
$K\alpha$	S	S	Y	S	S	S	. . .	Y	S	Y	S	Y	. . .	S	S	S	. . .
$K\beta$	Y	Y	W	S	Y	Y	. . .	Y	S	Y	S	W	. . .	S	S	S	. . .
66.2	. . .	. . .	. . .	. . .	. . .	. . .	. . .	. . .	. . .	. . .	W	. . .	. . .	. . .	W	. . .	. . .
71.5	Y	Y	. . .	S	. . .	Y	. . .	. . .	Y	. . .	S	. . .	. . .	. . .	Y	Y	. . .
73.1	VW	VW	. . .	. . .	. . .	. . .	. . .	. . .	VW	. . .	W/Y	. . .	. . .	. . .	. . .	. . .	. . .
90.8	. . .	. . .	. . .	. . .	. . .	. . .	. . .	. . .	. . .	. . .	. . .	. . .	. . .	W/Y	. . .	. . .	. . .
93.4	. . .	. . .	. . .	Y	. . .	. . .	. . .	. . .	. . .	. . .	. . .	. . .	. . .	. . .	. . .	. . .	. . .
99.1	. . .	. . .	. . .	. . .	. . .	. . .	. . .	. . .	. . .	. . .	. . .	. . .	. . .	. . .	Y	. . .	. . .
104.9	. . .	. . .	. . .	. . .	. . .	. . .	. . .	. . .	. . .	. . .	. . .	. . .	. . .	. . .	VW	. . .	. . .
112.9	. . .	. . .	. . .	Y	S	. . .	. . .	. . .	. . .	. . .	. . .	. . .	. . .	. . .	. . .	W	. . .
115.7	. . .	. . .	. . .	VW	. . .	. . .	. . .	. . .	. . .	. . .	. . .	. . .	. . .	. . .	. . .	. . .	. . .
116.2	. . .	. . .	. . .	VW	. . .	. . .	. . .	. . .	. . .	. . .	. . .	. . .	. . .	. . .	. . .	. . .	. . .
120.5	. . .	. . .	. . .	W	. . .	. . .	. . .	. . .	. . .	. . .	. . .	. . .	. . .	. . .	. . .	. . .	. . .
129.8	. . .	. . .	. . .	Y	. . .	. . .	. . .	. . .	. . .	. . .	. . .	. . .	. . .	W/Y	. . .	W	. . .
133.7	. . .	. . .	. . .	W	. . .	. . .	. . .	. . .	. . .	. . .	. . .	. . .	. . .	. . .	. . .	. . .	. . .
139.4	W	W	. . .	. . .	. . .	. . .	. . .	. . .	. . .	W/Y	Y	. . .	. . .	. . .	. . .	. . .	. . .
147.6	. . .	. . .	. . .	. . .	. . .	. . .	. . .	VW	. . .	. . .	. . .	. . .	. . .	. . .	. . .	. . .	. . .
153.4	. . .	. . .	W	Y	. . .	. . .	. . .	. . .	VW	. . .	. . .	. . .	. . .	. . .	. . .	. . .	. . .
169.7	. . .	. . .	. . .	VW	. . .	. . .	. . .	. . .	. . .	. . .	. . .	. . .	. . .	VW	. . .	. . .	. . .
171.8	. . .	. . .	. . .	VW?	. . .	. . .	. . .	. . .	. . .	. . .	. . .	. . .	. . .	. . .	. . .	. . .	. . .
182.0	. . .	. . .	. . .	VW?	. . .	. . .	. . .	. . .	. . .	. . .	VW?	. . .	. . .	. . .	. . .	. . .	. . .
183.0	. . .	. . .	. . .	. . .	. . .	. . .	. . .	. . .	. . .	. . .	. . .	. . .	. . .	VW	. . .	. . .	. . .
184.1	. . .	. . .	. . .	. . .	. . .	. . .	Y	. . .	. . .	. . .	. . .	. . .	. . .	. . .	. . .	. . .	. . .
185.3	. . .	. . .	. . .	W	. . .	. . .	. . .	. . .	. . .	. . .	. . .	. . .	. . .	W	. . .	. . .	. . .
192.2	. . .	. . .	W	S	. . .	. . .	. . .	. . .	Y	. . .	. . .	. . .	Y	. . .	. . .	VW	. . .
197.2	. . .	. . .	. . .	W/Y	. . .	. . .	. . .	. . .	. . .	. . .	. . .	. . .	. . .	. . .	. . .	. . .	. . .
199.9	. . .	. . .	. . .	VW	. . .	. . .	. . .	. . .	. . .	. . .	. . .	. . .	. . .	. . .	. . .	. . .	. . .
203.6	. . .	. . .	. . .	. . .	. . .	. . .	. . .	. . .	. . .	. . .	. . .	. . .	. . .	. . .	VW	. . .	. . .
214.1	. . .	. . .	. . .	. . .	. . .	. . .	. . .	. . .	. . .	. . .	Y	. . .	. . .	. . .	VW	. . .	. . .
216.9	. . .	. . .	. . .	. . .	. . .	. . .	. . .	. . .	. . .	. . .	. . .	. . .	. . .	. . .	. . .	. . .	W
222.1	. . .	. . .	. . .	W	. . .	. . .	. . .	. . .	. . .	. . .	. . .	. . .	. . .	VW	. . .	. . .	. . .
225.4	. . .	. . .	W	. . .	. . .	. . .	. . .	. . .	S	. . .	. . .	Y	. . .	S	. . .	. . .	. . .

TABLE II. (*Continued*).

Coincident lines	Energy window on high energy lines																
	214.1	219.2	222.1	225.4	227.9	233.7	240.7	251.2	262.6 263.7	277.6	284.6	299	301	310.1	335.8	422.6 425.3 425.8	563.9 565.2
236.0	...	...	...	...	...	...	...	...	...	...	...	...	...	...	VW	...	...
238.6	...	...	...	W	...	...	...	...	...	...	...	...	...	...	...	...	...
251.2	...	...	...	...	...	...	...	...	W	...	...	...	...	...	Y	...	...
262.6+	...	...	...	(W)	...	...	...	...	...	...	...	...	...	...	...	...	...
263.7	...	...	VW	Y	...	...	...	...	VW?	...	...	...	W/Y	...	...	...	...
264.7	...	...	...	...	...	...	...	...	...	...	W	...	...	...	...	...	...
271.8	...	...	...	...	...	...	...	...	W	...	...	...	...	...	...	...	...
274.7	...	...	...	...	...	...	...	...	...	...	...	...	...	...	...	...	Y
284.6	Y	...	...	...	...	...	...	...	W	...	...	...	...	...	...	...	...
299.4	...	...	...	W	...	...	...	...	...	...	...	...	...	...	...	...	...
301.7	...	...	...	VW	...	...	...	...	...	...	...	...	...	...	...	...	...
306.0	...	...	...	...	...	...	...	...	...	...	...	...	...	...	...	...	VW
309.1	...	...	...	...	...	...	W	...	...	...	...	...	...	...	...	...	...
310.1	...	...	...	S	...	...	...	...	VW	...	W	...	...	...	...	...	...
320.6	...	...	...	VW?	...	...	...	...	...	...	...	...	...	...	...	...	...
330.5	...	...	...	...	...	...	...	...	...	...	...	...	...	VW	...	...	...
335.8	VW?	...	...	...	...	...	...	Y	...	...	...	...	...	...	...	...	...
338.0	...	...	...	...	...	...	...	...	...	...	...	...	...	...	VW	...	...
350.3	...	...	...	...	...	...	...	...	...	...	...	...	...	...	W	...	...
362.2	...	...	...	...	...	...	...	...	...	...	VW	...	...	...	...	...	...
392.6	...	...	...	...	...	...	...	...	...	...	...	VW?	...	...	...	...	...
419.6	...	...	...	...	VW	...	...	...	...	...	...	...	...	...	...	...	...
424.5	...	...	...	...	...	...	...	...	VW?	...	...	...	...	W	...	...	...
433.3	...	...	...	...	...	...	...	...	VW?	...	...	...	...	...	...	...	...
439.6	...	...	...	...	...	...	...	...	...	...	...	...	...	...	VW	...	...

The most relevant results of the coincidence measurement are compiled in Table II, which lists the coincident transitions to all gamma rays that have been selected by energy windows. The classification of the coincidences has been adopted from Minor *et al.* [16] (see caption of Table II). A complementary table for the energy windows defined by the planar detector is given in Ref. 34.

E. Lifetime measurements

Previous lifetime measurements in the ^{175}Lu$(n,\gamma)^{176}$Lu reaction [36] have led to the identification of 3 ns isomers in ^{176}Lu. The present experiment was carried out at the end position of a neutron guide at the ILL high flux reactor. Compared to the previous study, much better statistics could be achieved with an improved setup consisting of a BaF_2 scintillator and a 20% HPGe detector for recording delayed γ-γ coincidences from the ^{175}Lu$(n,\gamma)^{176}$Lu reaction. The overall time resolution was $\sim$4 ns.

The measured time distributions were analyzed by means of the generalized centroid-shift method, another improvement with respect to Ref. [36]. Thereby, windows are set on full-energy peaks as well as on Compton background positions. The net time distributions of the full-energy peaks are ascertained by interpolation between two distributions obtained with windows on neighboring Compton background positions, respectively. The centroids (first moments) of the full-energy peaks are plotted versus gamma-ray energy as a centroid diagram, where the centroids of prompt transitions form the zero-time line. Deviations from that line indicate delayed transitions, the deviation being a direct measure of the (effective) mean lifetime τ. Possible delayed feeding from higher lying isomers has to be considered properly. A detailed discussion of this procedure can be found elsewhere (Ref. [37] and citations therein).

In Fig. 7, part of the centroid diagram of the present experiment is displayed. In the following, some of the level energies that are discussed in the subsequent sections are used in advance to derive the respective lifetimes. The centroids of the 251.2 keV and the 350.4 keV transitions, which clearly appear above the zero-time line, are deexiting the 4^+ level at 985.6 keV [Fig. 8(l)], indicating a half life of

$$t_{1/2}(985.6\ \text{keV}) = 1.2 \pm 0.3\ \text{ns}\ .$$

Similarly, the centroid shifts of the 660.8 keV and 727.1 keV transitions depopulating the 3^- level at 960.2 keV [Fig. 8(j)] yield a half life of

$$t_{1/2}(960.2\ \text{keV}) = 0.7 \pm 0.2\ \text{ns}\ .$$

Furthermore, the half life of the 5^+ level at 657.1 keV [Fig. 8(i)] can be estimated to

$$t_{1/2}(657.1\ \text{keV}) < 0.5\ \text{ns}$$

using the centroid shift of the 284.6 keV transition and by considering delayed feeding from higher lying isomers. For the astrophysical aspects (see paper II), the half lives of the levels at 838.6 and 921.5 keV [Figs. 8(f) and (e)] are particularly important. From the centroid positions of the corresponding ground state transitions, upper limits

$$t_{1/2}(838.6\ \text{keV}) < 0.3\ \text{ns}$$

and

$$t_{1/2}(921.5\ \text{keV}) < 0.2\ \text{ns}$$

can be set.

Another relevant level in this context is the 4^- bandhead at 722.9 keV [Fig. 8(f)], which can influence the time constant for equilibration of ground state and isomer in the stellar plasma provided that its half-life is in the ns range. A determination of this lifetime is complicated, since the 722.9 keV level decays mainly by a highly converted transition to the 3^- level at 658.4 keV. The effective half-life of the latter was determined to 6.3 ± 0.5 ns [36]. From the delayed gamma-ray spectrum (Fig. 1 in Ref. [36]) one concludes, however, that the lifetime of the 722.9 keV level must be considerably shorter; otherwise, the 218.0 keV transition from the 722.9 keV level should exhibit a similar delay, comparable to that of the 153.6 and 271.9 keV transitions from the 658.4 keV level. Nevertheless, the present data do not exclude a lifetime of 1 to 2 ns for the 722.9 keV state. The net time distribution of the strong 225.4 keV transition from the 658.4 keV level (that has been measured in this work with at least 10 times better resolution than in Ref. [36]) exhibits a complex character with a slightly higher half-life of $t_{1/2,\text{eff}} = 7.2$ ns and possible indications of delayed feeding. If the intensities of the relevant transitions are taken into account, this effective half-life can be fitted by a 6.5 ns half-life of the 658.4 keV state and a half-life of

$$t_{1/2} \leq 2\ \text{ns}$$

for the 722.9 keV level. This result appears plausible since all transitions depopulating this level are forbidden in first order (i.e., without configuration mixing, see following sections).

For the 658.4 keV state we obtain

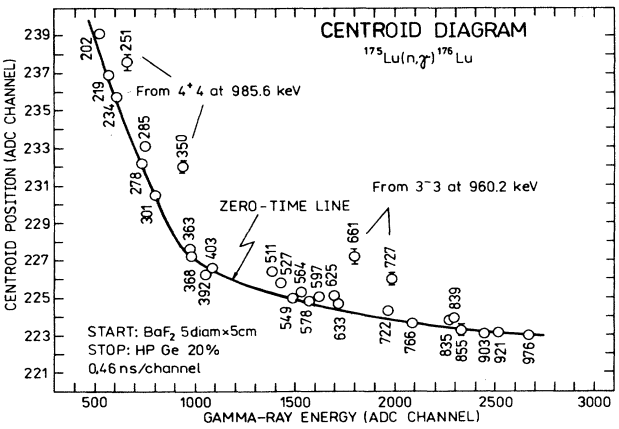

FIG. 7. Centroid-shift analysis of some time distributions obtained in the ^{175}Lu$(n,\gamma)^{176}$Lu reaction.

$t_{1/2}(658.4\ \text{keV}) = 6.5^{+0.3}_{-1.0}$ ns .

The larger uncertainty for the lower limit is due to possible delayed feeding from other higher-lying isomers. For the sake of completeness, we note that a half-life of 7.8±0.5 ns for the level at 635.2 keV was obtained, in good agreement with the previous measurement (8.0±1.0 ns) [36].

F. The ^{175}Lu$(d,p)^{176}$Lu experiment

For the unambiguous assignment of gamma transitions between levels related to the ground state and to the isomer, it is mandatory to define the isomer energy as precise as possible. To this end, the results from the experiments at Grenoble are supplemented with data from a (d,p) measurement at the TU Munich.

The (d,p) transfer reaction was carried out at the Tandem accelerator of the University and the Technical University of Munich. A ^{175}Lu target was bombarded by deuterons of 20.118 MeV. The protons in the exit channel were analyzed under 45° with a Q3D spectrograph [38] and recorded with a multiwire detector [39] with 576 wires and a wire distance of 0.5 mm. Three energy regions were covered in different runs, and the resulting

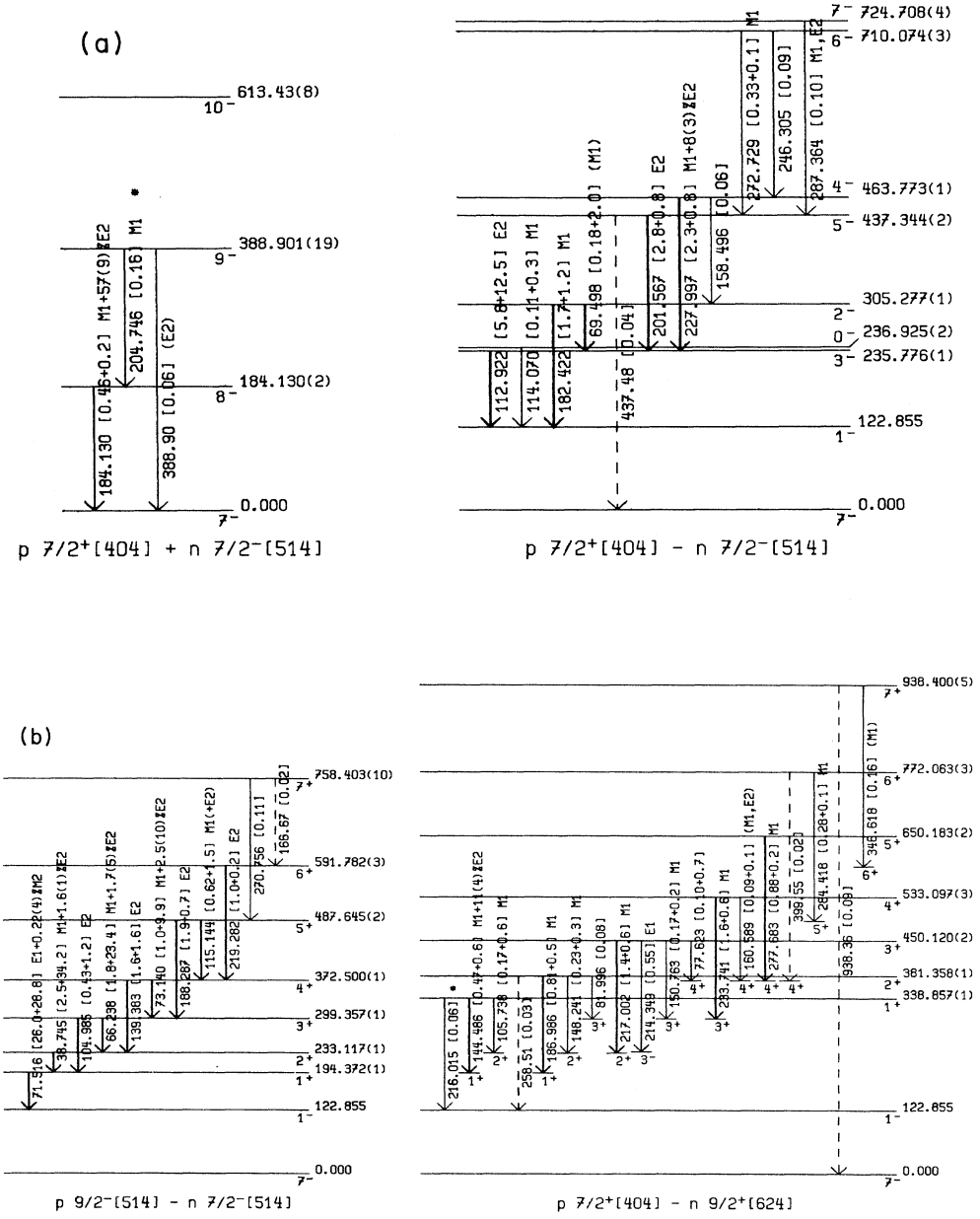

FIG. 8. The level scheme of ^{176}Lu.

proton spectra were calibrated by means of the known level energies (see Sec. VI A). In this measurement, a resolution of 3 to 4 keV in proton energy was obtained.

IV. CONSTRUCTION OF THE LEVEL SCHEME

A. The input data

The following input information has been used in establishing the level scheme.

(i) In total, 509 gamma transitions could be identified in the present measurements of the (n,γ) and (n,e^-) reactions on ^{175}Lu, including transition energies, intensities, and in many cases also the multipolarities. The energy precision achieved in these data is particularly important for an efficient application of the Ritz combination principle to the numerous transitions of the present study, and for reducing accidental assignments. A further reduction of accidental assignments is achieved by means of the transition multipolarities. The data from the $(\gamma\text{-}\gamma)$ coincidence measurement are useful for confirming or excluding assignments that are based on individual transitions. The information from the high resolution ^{175}Lu$(d,p)^{176}$Lu measurement was of key importance for the exact determination of the isomer energy, and hence for establishing the connection between the partial level

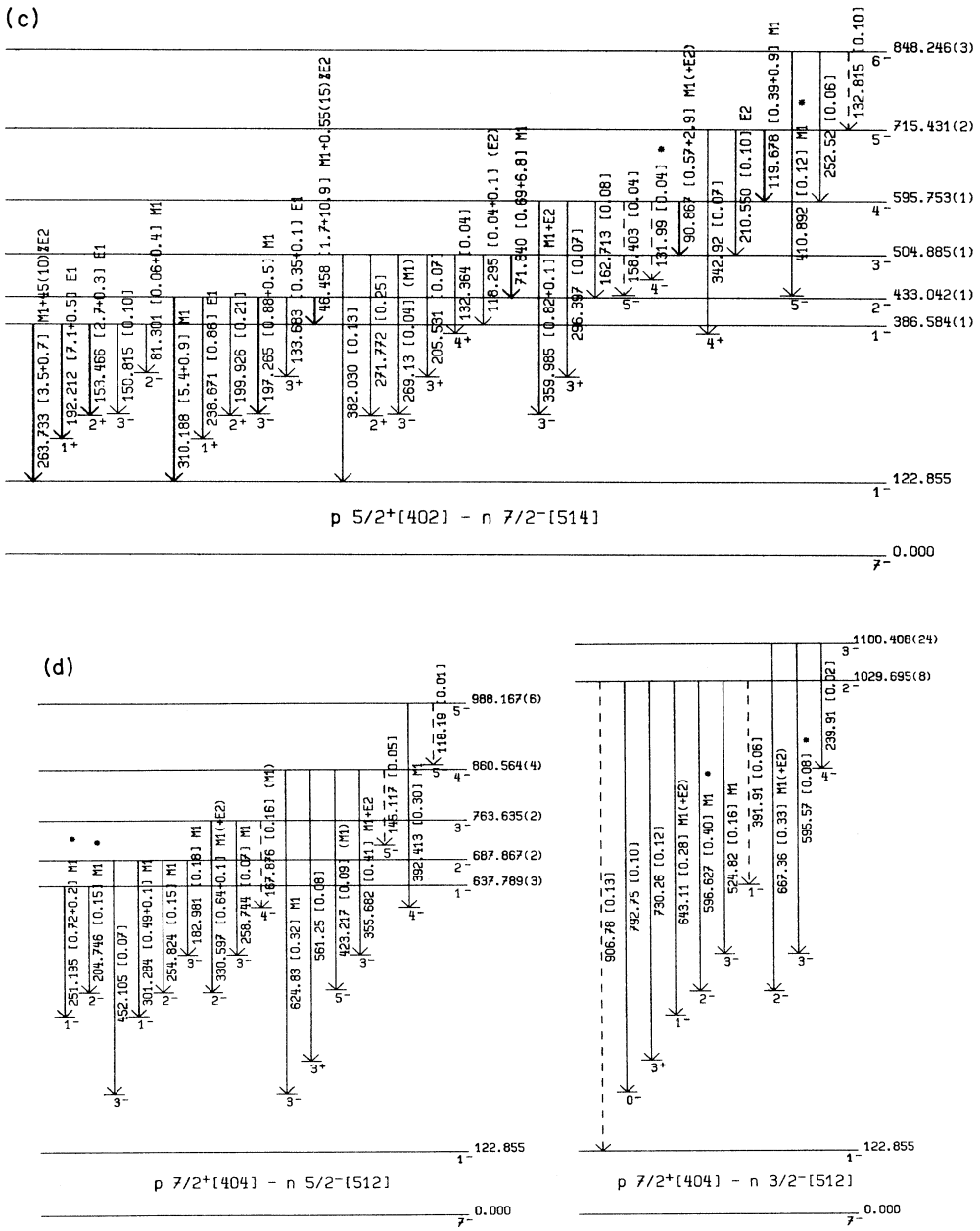

FIG. 8. (*Continued*).

schemes that refer to the ground state and isomer, respectively.

(ii) Data from the literature that have been used to complement the present work include the results from the $^{177}Hf(t,\alpha)^{176}Lu$ experiment of Dewberry *et al.* [20] as well as from Coulomb excitation studies [21,22]. Relevant information was also adopted from an investigation of primary gamma transitions following capture of epithermal neutrons [26]. The results from these average resonance capture (ARC) studies allowed the assignment of various levels in a well-defined spin and parity window, i.e., for levels with $2^- \leq I^\pi \leq 5^-$ in the energy range below 1100 keV. Though the resolution of this measurement was not sufficient to separate closely spaced levels,

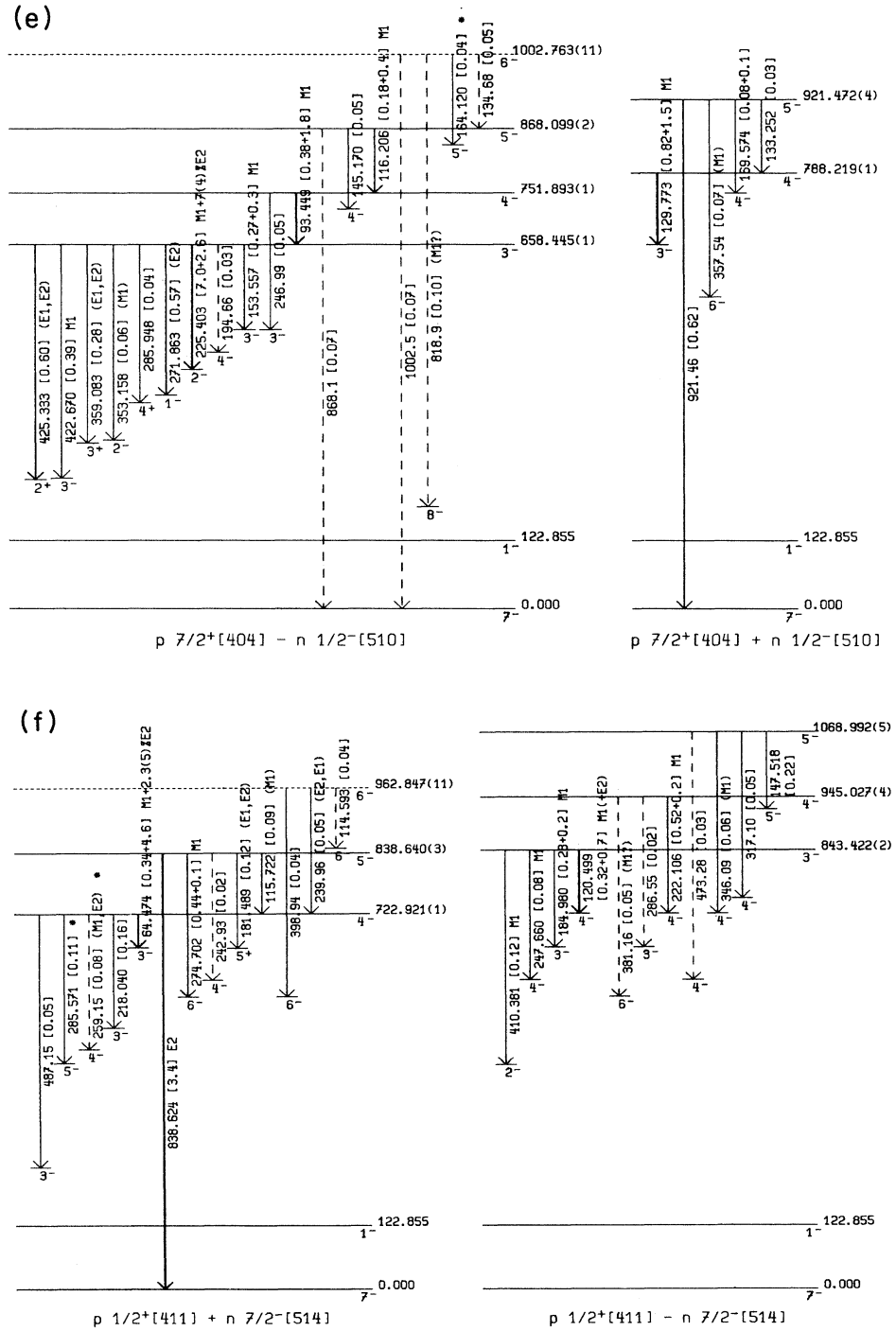

FIG. 8. (*Continued*).

these cases could be decided via the secondary transitions observed in the present measurements.

B. Principles

The level scheme was established in three steps.

(i) As in previous studies, two separate level schemes were constructed by means of the Ritz combination principle, which are built on the ground state and on the isomer, respectively. In both schemes, an excellent precision of 1 to 10 eV is achieved for the level energies, but the absolute energies of the second scheme remain uncertain due to the ~2 keV uncertainty of the isomer energy.

(ii) That energy could be defined with considerably improved accuracy from the spectrum of the (d,p) measurement, which was calibrated with the well-established GAMS data. In a second step, the isomer energy was fixed to high precision by several mediating transitions between the two schemes that were ultimately identified in the GAMS spectra.

(iii) The unified level scheme was checked for consistency with all other data. In this step, the scheme was further improved and extended.

For the construction and interpretation of the level scheme, the data from the ARC measurement of Hoff *et al.* [26] and from the (t,α) study of Dewberry *et al.* [20] are repeatedly cited. For easier comparison, these data are compiled in Table III together with the present (d,p) results and all the levels discussed in this work. The ARC data were renormalized from the previously postu-

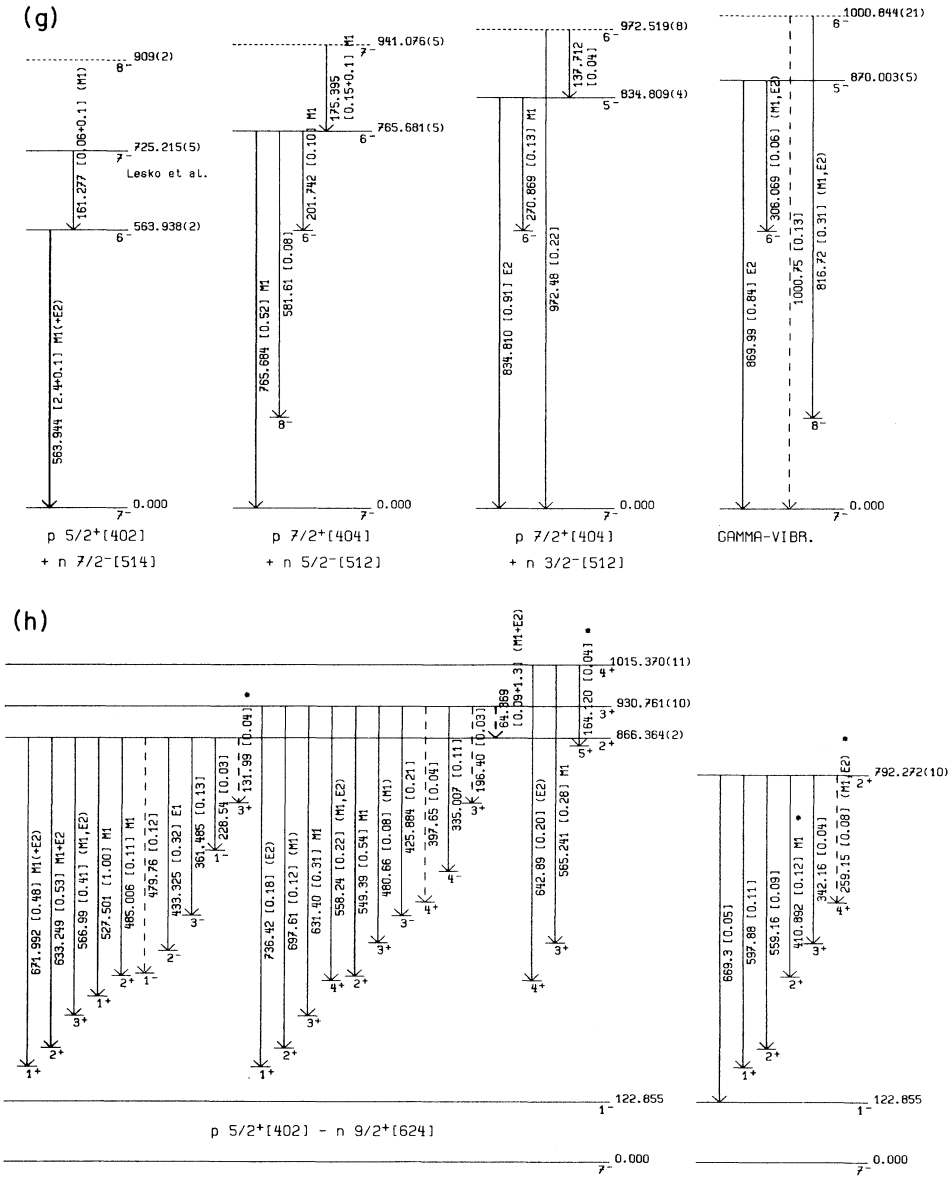

FIG. 8. (*Continued*).

lated isomer-energy of 126.500 keV [19] to the present result of 122.855 keV (Sec. V B). The corresponding reduction of the level energies of Hoff *et al.* [26] by 3.6 keV results in a remaining average systematic difference of 0.3 keV compared to the present level energies. This difference, which is comparable to the statistical uncertainties quoted by Hoff *et al.* [26], was corrected for as well so that the energies in Table III are 3.9 keV lower than given in Ref. [26]. In comparing the present level energies with those of Balodis *et al.* [19], a similar shift of $\Delta E = -3.645$ keV must be considered due to the revised energy of the isomeric state.

The revised energy scale can be used to derive an improved value for the neutron separation energy S_n of ^{176}Lu:

$$S_n = E_\gamma^{\text{prim}} + E_x - E_n \ ,$$

where E_γ^{prim} is the energy of a primary gamma-transition to a level E_x; the neutron energy for the ARC measurements with the scandium filter is $E_n = 2 \pm 0.5$ keV [40]. The ten strongest lines observed in the ARC measurements [26] then yield an average value

$$S_n = 6287.91 \pm 0.15 \text{ keV} \ .$$

The uncertainty is conservatively estimated to corre-

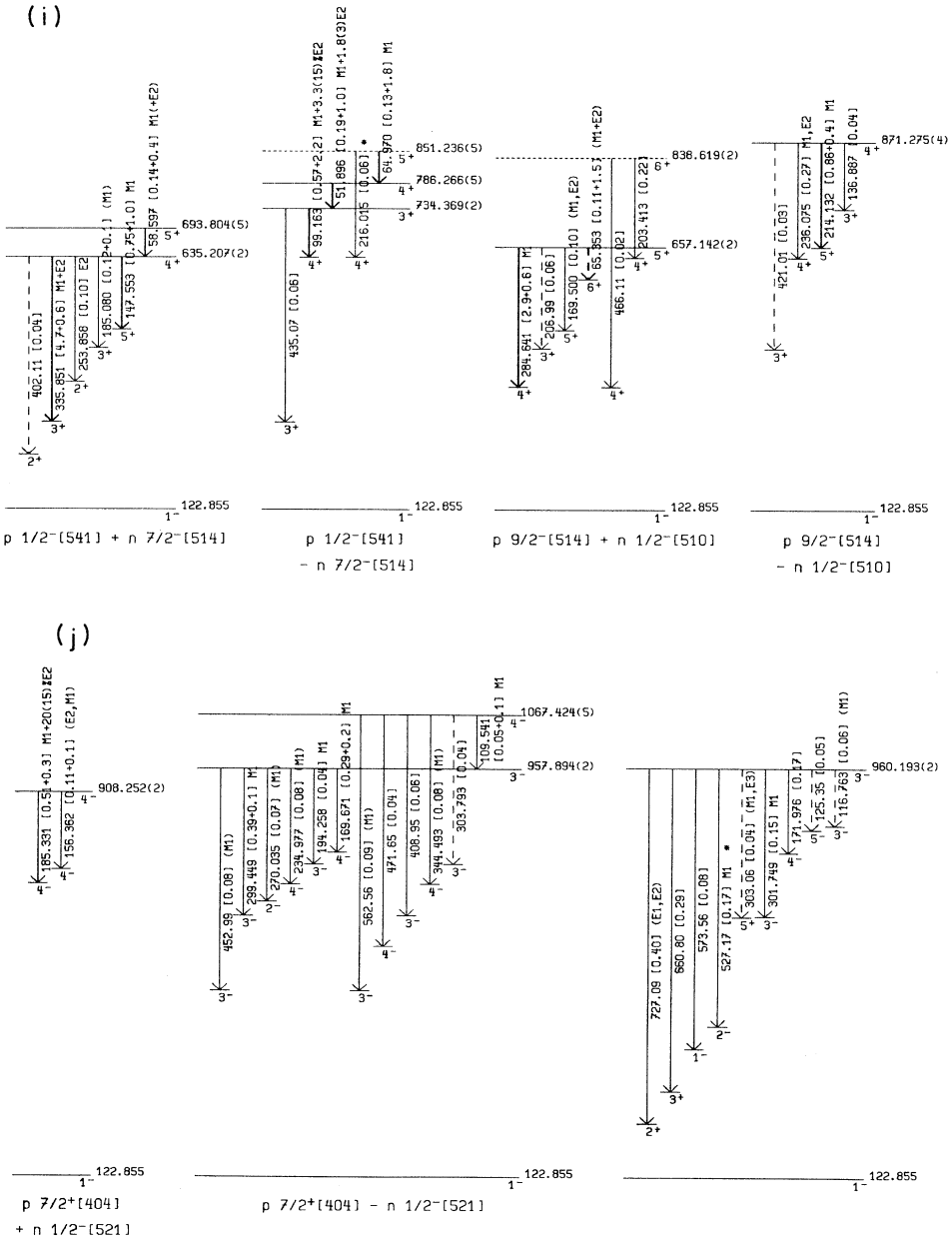

FIG. 8. (*Continued*).

spond to one third of the neutron energy spread. This result is significantly smaller than the value of 6289.5 keV given by Browne [41].

The entire level scheme of ^{176}Lu is presented in Figs. 8(a) to (m), ordered in rotational bands with the configuration assignments as discussed below. The level energies (in keV) are given with their respective statistical uncertainties. Assigned gamma transitions are indicated by vertical arrows; the transition energies (in keV) are followed in brackets by the gamma intensities and—if determined—by the conversion electron intensities. The latter were calculated via the *theoretical* conversion coefficients obtained from the experimental multipolarities. Multiply assigned transitions are marked by (*). Transitions indicated by dashed lines are either characterized by poor statistics or are contaminated by lines from neighboring nuclei; uncertain levels are also shown as dashed lines.

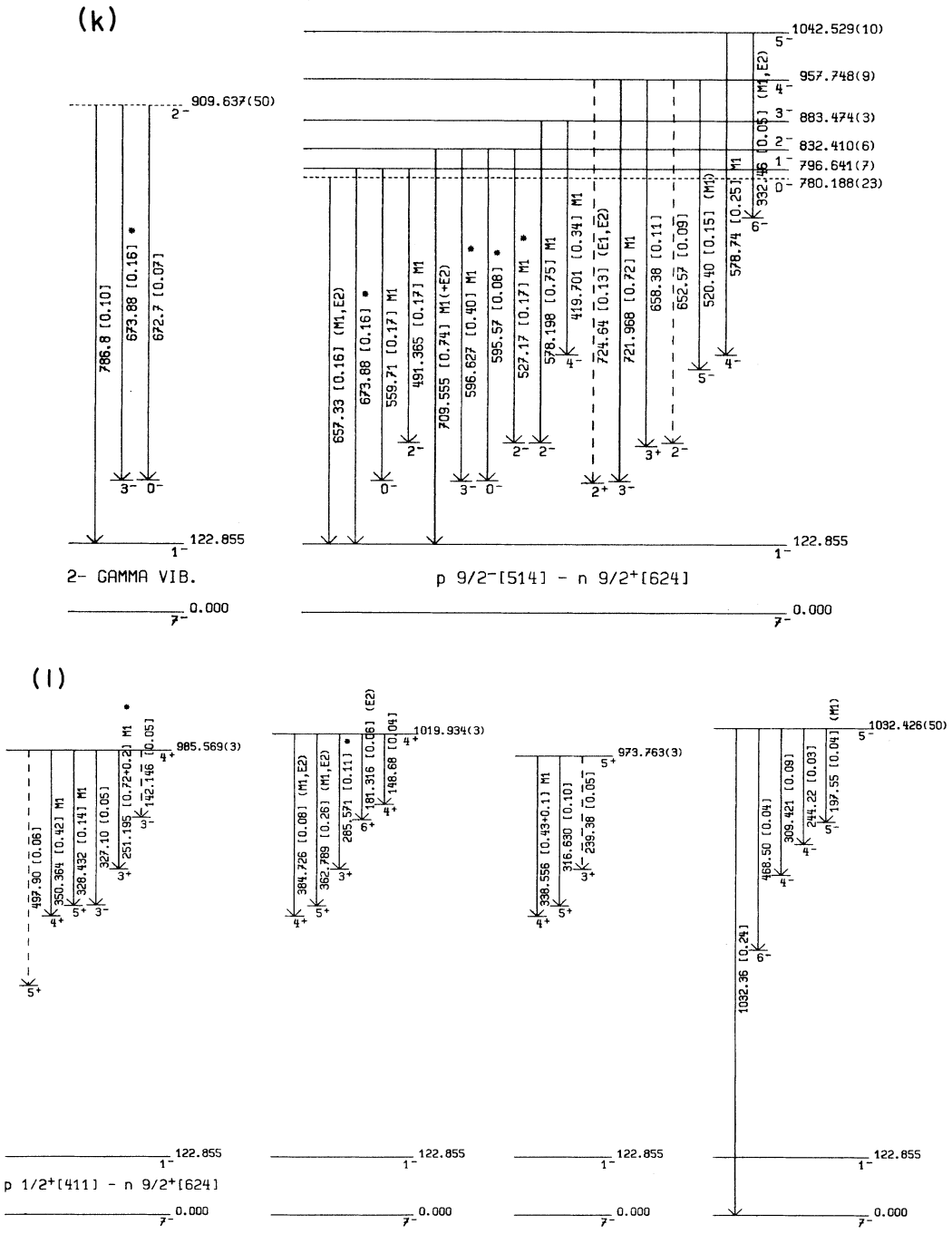

FIG. 8. (*Continued*).

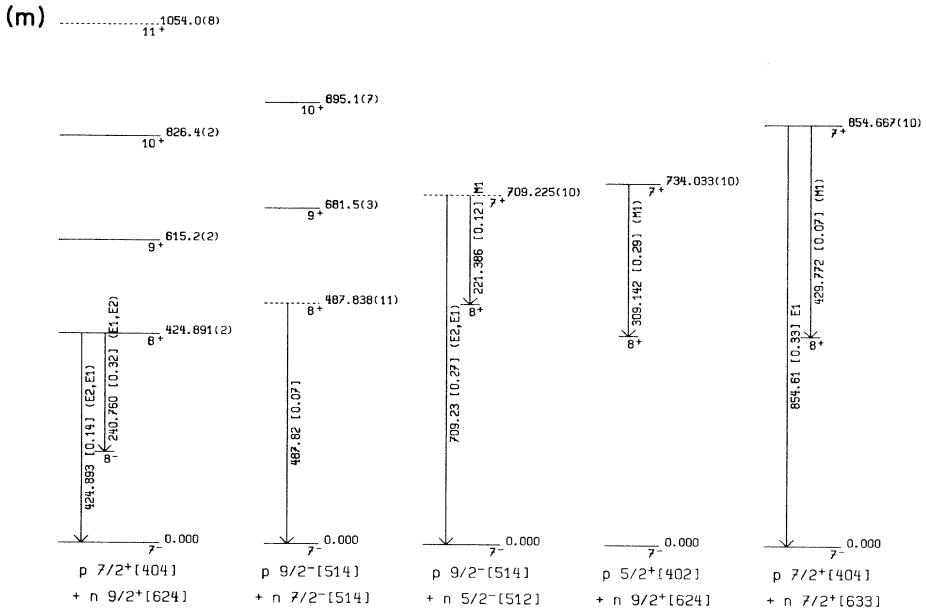

FIG. 8. (*Continued*).

C. Uncertainties of the level energies

In the level scheme presented in Figs. 8(a) to (m), energies are given with statistical uncertainties, since this is the relevant aspect in connection with the Ritz combination principle. If absolute uncertainties are of interest, there are two additional contributions that need to be considered.

(i) The isomer energy carries a statistical uncertainty of 6 eV. This uncertainty is larger than the internal precision of the partial level scheme built on the isomer and needs to be added to the quoted uncertainties.

(ii) A more significant uncertainty arises from the calibration of the GAMS data to the energy of the $K\alpha_2$ x-ray line of lutetium, $E_x = 52.9650$ keV [31]. Since the energy scale can be renormalized by multiplication of all energies with a constant factor, the estimated 3 eV uncertainty of the x-ray line translates into a systematic uncertainty for all gamma transitions and level energies of

$$\frac{\Delta E}{E} = 5.7 \times 10^{-5} .$$

While this effect contributes only 7 eV to the uncertainty of the isomer energy, it amounts to 45 eV at energies around 800 keV, and hence exceeds several times the statistical uncertainties. These systematic uncertainties are considered in the results presented in Table III.

V. CONFIRMATION OF KNOWN LEVELS

A. Rotational bands and levels from previous (n,γ) studies

The well-established part of the level scheme of Balodis *et al.* [19] contains five rotational bands with $K^\pi = 0^-$, 1^+, 1^+, 1^-, and 1^-. These will be discussed with respect to their experimental confirmation and to some changes in their assignment. A detailed presentation of the energy sequence in these bands and the resulting rotational parameters may be found in Ref. [19]. From the less well established bands [16,19] only those with $K^\pi = 3^-$, and 4^- are discussed, since these are important for the coupling of isomer and ground state. The 4^+ and 5^+ levels [19] are dealt with in the context of the extension of the level scheme.

The $K^\pi = 0^-$ band; $p\frac{7}{2}^+[404]$-$n\frac{7}{2}^-[514]$. All members of this band from $I^\pi = 0^-$ to 7^- were confirmed [Fig. 8(a)]. The weakly established 114 keV transition from the 0^- bandhead to the 1^- level could be confirmed by the measured multipolarity $M1$. The 1^- to 5^- members of this band were already well established by coincidences, multipolarities and energy combinations. The decay of the 6^- member could be confirmed by the unambiguous assignment of the 272 keV transition, which has now also the correct multipolarity $M1$. The 7^- member is confirmed by the multipolarity of the 287 keV transition.

The $K^\pi = 1^+$ band at 194.372 keV; $p\frac{9}{2}^-[514]$-$n\frac{7}{2}^-[514]$. For this band, the previously known members $I^\pi = 1^+$ to 6^+ were confirmed [Fig. 8(b)]. The suggested 7^+ member is based on the well-established energy systematics [19] and on the combination of two weak transitions. The change in the Nilsson configuration will later be justified in connection with the transition systematics in other bands.

The $K^\pi = 1^+$ band at 338.857 keV; $p\frac{7}{2}^+[404]$-$n\frac{9}{2}^+[624]$. This band is characterized by the absence of intraband transitions. The strongest transitions from all levels occur to the neighboring band with $K^\pi = 1^+$ [Fig. 8(b)]. The 1^+ to 5^+ members of Balodis *et al.* [19] were confirmed via the transitions to the $K^\pi = 1^+$ band, but two suggested weak intraband transitions could not be detected. The 6^+ level of Balodis *et al.* [19] was tenta-

TABLE III. The energy levels in ^{176}Lu obtained in this work together with results from a (t,α) measurement [20] and an ARC measurement [26]. For the (t,α) measurement all data are quoted as given in Ref. [20]; assignments for I^π, K that do not agree with this work are marked by (?). The level energies of the ARC data (Ref. [26]) are renormalized by $\Delta E = -3.9$ keV as described in the text; the comment C: $I^\pi + I^\pi$ means that the ARC measurement confirms earlier assignments; the ARC data are then compatible with other I^π assignments as well.

^{177}Hf$(t,\alpha)^{176}$Lu (Ref. [20])				^{175}Lu$(d,p)^{176}$Lu		ARC (Ref. [26])		^{175}Lu$(n,\gamma)^{176}$Lu and ^{175}Lu$(n,e^-)^{176}$Lu		
E (keV)	Intensity	I^π	K	E (keV)	Intensity	E (keV)	I^π	E (keV)	I^π	K
0±1	0.0306	7^-	7					0.000±0.000	7^-	7
123±1	0.0099	1^-	0	122.9±0.4	2.3			122.855±0.009	1^-	0
184±3	0.0004	8^-	7	183.9±0.3	5.6			184.130±0.011	8^-	7
198±3	0.0001	1^+	1					194.372±0.013	1^+	1
233±4	0.0003	2^+	1					233.117±0.015	2^+	1
						235.5±0.3	3^-	235.776±0.015	3^-	0
240±2	0.0096	3^-	0	235.9±0.3	5.3			236.926±0.015	0^-	0
301±1	0.0060	3^+	1	299.3±1.4	1.2	299.7±0.3	3^+	299.357±0.018	3^+	1
308±1	0.0130	2^-	0	305.2±0.6	3.7	305.5±0.3	2^-	305.277±0.018	2^-	0
				338.6±0.7	0.5			338.856±0.020	1^+	1
				372.7±0.3	2.8	372.1±0.3	4^+	372.500±0.022	4^+	1
377±4	0.0041	2^+	1			380.8±0.5	2^+	381.358±0.023	2^+	1
								386.584±0.023	1^-	1
391±3	0.0106	1^-	1	387.1±0.6	1.9			388.901±0.029	9^-	7
				425.1±0.7	3.1			424.891±0.024	8^+	8
						433.7±0.3	2^-	433.042±0.025	2^-	1
433±1	0.0118	2^-	1	435.8±0.6	2.9	438.2±0.4	5^-	437.344±0.026	5^-	0
459±7	0.0049	3^+	1	450.6±0.6	1.6	449.7±0.3	3^+	450.121±0.026	3^+	1
				463.9±0.4	3.8	463.8±0.3	4^-	463.773±0.027	4^-	0
						487.2±0.4	5^+	487.645±0.028	5^+	1
486±3	0.0085	8^+	8	487.9±0.3	4.0			487.838±0.030	8^+	8
505±2	0.0069	3^-	1	504.7±0.3	2.1	504.9±0.3	3^-	504.885±0.029	3^-	1
538±3	0.0023	4^+	1	532.8±0.3	2.6	533.2±0.3	4^+	533.097±0.031	4^+	1
565±3	0.0324	6^-	6					563.938±0.032	6^-	6
								591.782±0.034	6^+	1
594±3	0.0028	4^-	1	593.4±0.7	3.0	595.6±0.3	4^-	595.753±0.035	4^-	1
607±10	0.0024			615.1±0.3	6.8				9^+	8
						635.0±0.3	$3^+,4^+$	635.207±0.037	4^+	4
				637.5±0.5	1.3			637.789±0.037	1^-	1
653±6	0.0059			650.4±0.9	2.8	649.8±0.8	5^+	650.183±0.038	5^+	1
						658.1±0.3	C: 3^-+5^+	657.142±0.038	5^+	5
				658.4±0.2	67.9			658.445±0.038	3^-	3
683±3	0.0132	9^+	8	681.7±0.6	2.8				9^+	8
				688.2±0.3	4.3			687.867±0.040	2^-	1
						687.8±0.3	C: $2^-+3^+,4^+$	693.803±0.040	5^+	4
								709.225±0.042	7^+	7
				711.1±1.0	1.5			710.073±0.041	6^-	0

TABLE III. (*Continued*).

^{177}Hf(t,α)^{176}Lu (Ref. [20])			^{175}Lu(d,p)^{176}Lu		ARC (Ref. [26])		^{175}Lu(n,γ)^{176}Lu and ^{175}Lu(n,e^-)^{176}Lu		
E (keV)	Intensity	I^π K	E (keV)	Intensity	E (keV)	I^π	E (keV)	I^π	K
					715.1±0.3	C: $3^+,4^+ + 5^-$	715.432±0.041	5^-	1
			722.6±0.3	4.7	722.8±0.3	$4^-(+2^-,5^-)$	722.921±0.042	4^-	4
723±2	0.0730	4^- 4					725.215±0.042	7^-	6
							724.707±0.042	7^-	0
							734.033±0.042	7^+	7
					733.6±0.3	$3^+,4^+$	734.369±0.042	3^+	3
757±4	0.0067	7^- 6?	751.8±0.2	51.5	751.7±0.3	4^-	751.893±0.043	4^-	3
							758.403±0.045	7^+	1
					763.4±0.3	3^-	763.635±0.044	3^-	1
			765.3±0.3	17.4			765.681±0.044	6^-	6
772±8	0.0020						772.063±0.045	6^+	1
							780.189±0.051	0^-	0
							786.266±0.045	4^+	3
789±4	0.0020		788.4±0.2	100.0	788.2±0.3	$3^-,4^-(+2^-,5^-)$	788.219±0.045	4^-	4
							792.265±0.049	2^+	
							796.641±0.046	1^-	0
			826.9±0.5	8.5				10^+	8
					833.5±0.3	$3^-(+2^-,5^-)$	832.410±0.048	2^-	0
			835.2±0.3	22.6			834.809±0.048	5^-	5
							(838.619±0.048)	(6^+	5)
840±2	0.0716	3^- 3			842.9±0.3	$3^-,4^- + 2^-,5^-$	838.640±0.048	5^-	4
							843.421±0.048	3^-	3
							848.248±0.049	6^-	1
							851.236±0.049	5^+	3
							854.667±0.050	7^+	7
			860.1±0.8	4.2	860.6±0.3	4^-	860.564±0.050	4^-	1
							866.367±0.050	2^+	2
864±6	0.0360	5^- 4?					868.099±0.050	5^-	3
			869.5±0.2	53.6	868.9±0.3	C: $5^- + 3^+,4^+$	870.003±0.050	5^-	5
							871.275±0.050	4^+	4
					883.1±0.3	$3^-,4^-$	883.474±0.051	3^-	0
889±10	0.0019		895.4±0.8	2.6				10^+	8
					903.1±0.3	$3^-,4^-;2\times2^-,5^-$			
			908.1±0.6	4.5			908.252±0.052	4^-	4
					907.6±0.3	$3^-,4^-(+2^-,5^-)$	(909.610±0.096)	(2^-	2)
909±2	0.0164	(2^- 2)							
			921.7±0.2	72.8	921.9±0.3	$2^-,5^-$	921.472±0.053	5^-	4
					929.5±0.8	$5^+,(2^+)$	930.761±0.054	3^+	2
							938.400±0.054	7^+	1
			941.8±0.3	17.1			941.076±0.054	7^-	6

TABLE III. (*Continued*).

^{177}Hf(t,α)^{176}Lu (Ref. [20])			^{175}Lu(d,p)^{176}Lu		ARC (Ref. [26])		^{175}Lu(n,γ)^{176}Lu and ^{175}Lu(n,e^-)^{176}Lu	
E (keV)	Intensity	I^π K	E (keV)	Intensity	E (keV)	I^π	E (keV)	I^π K
945±2	0.0411	4^- 3			944.9±0.3	4^-	945.027±0.054	4^- 3
					958.5±0.3	$3\times3^-,4^-$	957.748±0.056	4^- 0
			958.8±2.3	8.7			957.894±0.055	3^- 3
						or $4\times2^-,5^-$	960.193±0.055	3^- 3
966±3	0.0094	$(3^-$ 2)?					962.848±0.056	6^- 4
			971.8±2.3	8.2			972.519±0.056	6^- 5
					973.3±0.4	$5^+,(2^+)$	973.763±0.056	5^+ 5
							985.569±0.057	4^+ 4
			988.1±1.9	2.2	988.1±0.3	$3^-,4^-;2\times2^-,5^-$	988.167±0.057	5^- 1
							1000.844±0.061	6^- 5
			1000.4±2.3	25.3				
1006±3	0.0041						1002.784±0.066	6^- 3
							1015.370±0.059	4^+ 2
					1017.9±0.3	$3^+,4^+$	1019.934±0.059	$4^+,5^+$
			1029.6±0.3	21.2			1029.695±0.059	2^- 2
					1031.0±0.3	$3^-,4^-$	1032.382±0.063	5^- 5
1032±4	0.0060	6^- 4?						
					1042.2±0.3	$3^-,4^-,(2^-,5^-)$	1042.529±0.061	5^- 0
					1053.9±0.3	$3^-,4^-+2^-,5^-$		
1057±8	0.0130		1054.1±0.9	3.3				$(11^+$ 8)
			1062.7±0.4	15.6	1062.4±0.8	$2^-,5^-$		
							1067.424±0.061	4^- 3
					1068.1±0.3	$3^-,4^-(+2^-,5^-)$	1068.992±0.061	5^- 3
1074±5	0.0134	5^- 3	1071.7±0.3	25.5				
					1079.9±0.3	$5^-,(2^-)$		
			1100.4±0.3	21.8	1100.6±0.3	$3^-,4^-;2\times2^-,5^-$	1100.408±0.067	3^- 2

tively based on a combination of an interband and an intraband transition, but the interband transition could be rejected by the measured multipolarity of $E1$ or $E2$. Instead, another combination is suggested with the assignment of the 7^+ member being based on the energy systematics [19] and on a weak $M1$ transition to the 6^+ level in the neighboring band. However, contrary to the 1^+ to 5^+ members, the 6^+ and 7^+ levels have to be considered as less well established.

For the first time, transitions to the $K=0$ band could be assigned with the $3^+ \rightarrow 3^-$ transition being confirmed by the measured multipolarity $E1$. The occurrence of such $E1$ transitions to the $K=0$ band supports the tentative assignment of a 938 keV transition from the 7^+ level to the 7^- ground state, since the Nilsson configurations of the $K=0$ and $K=7$ band are identical. On the other hand, such a $7^+ \rightarrow 7^-$ transition violates the K selection rule, so that this assignment seems to be very uncertain.

The $K^\pi=1^-$ band at 386.584 keV; $p\frac{5}{2}^+[402]$-$n\frac{7}{2}^-[514]$. The members with $I^\pi=1^-$ to 6^- were established by Balodis *et al.* [19] and the Nilsson configuration was assigned by Dewberry *et al.* [20] on the basis of the population in the (t,α) reaction. All levels were clearly confirmed with the improved energy systematics and with the coincidence data [Fig. 8(c)].

The $K^\pi=1^-$ band at 637.789 keV; $p\frac{7}{2}^+[404]$-$n\frac{5}{2}^-[512]$. Also for this band, the levels were established by Balodis *et al.* [19], and the Nilsson configuration was assigned by Dewberry *et al.* [20]. The members from $I^\pi=2^-$ to 4^- could be clearly confirmed [Fig. 8(d)], but none of the reported weak intraband transitions was found in this work. The rather uncertain 5^- level can now be based on the $M1$ multipolarity of the 392 keV transition.

The $M1$ transitions depopulating the 1^- bandhead are very likely unresolved doublets. The 251 keV line appears in coincidence with the 153, 192, and 263 keV transitions, which all depopulate the 1^- level at 386 keV, and is hence identified as a $1^- \rightarrow 1^-$ transition. However, due to the also observed coincidence with the lines at 99 and 214 keV, part of its intensity must originate from a $4^+ \rightarrow 3^+$ transition, which will be discussed below. The additional and also well-established assignment for the 204 keV transition is part of the ground state band [21]. Therefore, the 1^- bandhead is less depopulated than suggested by the measured intensities of these two lines. A weak population of this bandhead is certainly plausible due to the absence of measured intraband transitions, and since no significant primary gamma transitions are to be expected in view of the spin difference to the 3^+ and 4^+ of the compound states.

The Nilsson configurations of the $K^\pi=1^+$ bands. The Nilsson configurations of the 1^+ bands have been exchanged compared to those of Balodis *et al.* [19] [Fig. 8(b)], according to the transition systematics of the 1^- bands, the configurations of which had been revised by Dewberry *et al.* [20]. In the 1^- band with $p\frac{5}{2}^+[402]$-$n\frac{7}{2}^-[514]$, there is a strong branching to the 1^+ band at 194.37 keV. The $E1$ transitions to this band are observed even in competition with the collective intraband transitions [Fig. 8(c)]. However, such high transition probabilities can only be expected if only one of the particle states is changed. Therefore, a

$$p\tfrac{9}{2}^-[514]\text{-}n\tfrac{7}{2}^-[514]$$

configuration for this 1^+ band is more likely, interpreting the observed gamma lines as odd $p\frac{5}{2}^+[402] \rightarrow \frac{9}{2}^-[514]$ transitions. The transition systematics of the 1^- band is then consistent with the results for the neighbor isotope ^{177}Lu [18], where odd proton states are the only single particle excitations. From the rotational band built on the $\frac{5}{2}^+[402]$ state, $M1$ transitions to the $\frac{7}{2}^+[404]$ ground state as well as competing transitions to the $\frac{9}{2}^-[514]$ state are observed in that nucleus.

In the neighboring isotopes, $\frac{9}{2}^-[514] \rightarrow \frac{7}{2}^+[404]$ transitions are strongly hindered, and a correspondingly large half-life of 35 ns was found for the 71.5 keV decay line of the 1^+ bandhead at 194.37 keV [36]. The hindrance of that $E1$ transition is confirmed by the 0.22(4)%$M2$ admixture observed in this work. An $M2$ transition between the configurations [514] and [404] is allowed by the selection rules of Alaga, but not the $E1$ transition in spite of its much higher single particle transition rate. $M2$ admixtures to the odd proton $[514] \rightarrow [404]$ $E1$ transitions were found in ^{175}Lu and ^{177}Lu as well.

For the $K^\pi=1^+$ band built on the 338.86 keV state, the modified assignments lead to the Nilsson configuration

$$p\tfrac{7}{2}^+[404]\text{-}n\tfrac{9}{2}^+[624] \ .$$

Already, Balodis *et al.* [19] noticed strong mixing between the configurations of the two 1^+ bands. The assigned Nilsson configurations represent the main part of the wave functions, but for a correct treatment the admixture from the neighboring band needs to be considered as well. This is in qualitative agreement with the weak population of *both* rotational bands in (d,p) transfer reactions, but the intensities are too small for a statement on transition mixing ratios.

The $K^\pi=3^-$ band at 658.445 keV; $p\frac{7}{2}^+[404]$-$n\frac{1}{2}^-[510]$. The 3^- bandhead was confirmed in the present study by a combination of nine transitions [Fig. 8(e)] with consistent spins and parities. The 4^- member is verified by a clear coincidence between the 93.4 and 225.4 keV lines, but the assignment of all higher energy transitions to this level by Balodis *et al.* [19] had to be abandoned in view of the present energy precision.

The tentative assignment of the 5^- member [19] could not be confirmed. Instead of the 118 keV transition, a line at 116.206 keV is now assigned as the intraband transition to the 4^- level, which exhibits also the correct multipolarity $M1$ and is in perfect agreement with the energy systematics of the 3^- and 4^- level spacing. According to Eq. (1), this band is characterized by a rotational parameter

$$A=\frac{\hbar}{2\Theta}=11.65(3) \text{ keV} \ .$$

Further, the new assignment is supported by the coincidence spectrum of the 225.4 keV line (the strongest transition depopulating the bandhead), where a weak signal of the 116.2 keV line was detected. The suggested 6^-

state is based on the combination of two weak gamma transitions in the expected energy region.

The $K^\pi=4^-$ bandhead at 722.921 keV; $p\frac{1}{2}^+[411]+n\frac{7}{2}^-[514]$. This level was proposed by Balodis *et al.* [19], and later confirmed by Dewberry *et al.* [20] as the bandhead of the above Nilsson configuration via an intense 723 keV line in the (t,α) spectrum. Figure 8(f) presents the now confirmed transitions. The strongest decay feeds the 3^- bandhead at 658.45 keV, but there is at least one K-forbidden transition to the $K=0$ band.

The $K^\pi=4^-$ bandhead at 788.219 keV; $p\frac{7}{2}^+[404]+n\frac{1}{2}^-[510]$. This level was postulated by Struble and Sheline [17] at ~791 keV on the basis of their (d,p) data. The assignment of two gamma transitions to that level [16] could not be confirmed by Balodis *et al.* Ref. [19]. The present data [Fig. 8(e)] show clearly that the 129.773 keV line is associated with the 4^- bandhead, in agreement with Minor *et al.* [16]; this assignment is supported by a coincidence with the 225.4 keV line and by multipolarity $M1$. A second depopulating transition in the scheme of Minor *et al.* [16] can be excluded, however.

A more detailed discussion of these 4^- bandheads will be given in Sec. VI B in connection with the mediating transitions between ground state and isomer.

B. Known levels coupled to the ground state

The ground state band $p\frac{7}{2}^+[404]+n\frac{7}{2}^-[514]$. Apart from the ground state, only a tentative assignment of the 8^- level at 185 keV was known from previous (n,γ) studies [16,19]. Since their spins differ significantly from the 3^+ and 4^+ compound spins, none of the members in this band is expected to be strongly populated in (n,γ) reactions.

However, the ground state band can be selectively populated by Coulomb excitation; in this way, it is possible to identify the corresponding gamma transitions even with limited energy resolution. The levels at 184.123(12), 388.83(2), and 613.43(8) keV could be assigned as the 8^-, 9^-, and 10^- members of the ground state band [21]. In this work, transitions from the 8^- and 9^- levels could be identified as well, in good agreement with Ref. [21] [Fig. 8(a)].

The $K^\pi=6^-$ bandhead at 563.94 keV; $p\frac{5}{2}^+[402]+n\frac{7}{2}^-[514]$. The bandhead was established by Dewberry *et al.* [20] from a strong line in the (t,α) spectrum in combination with the known gamma transition after neutron capture [19]; it is confirmed by the present multipolarity $M1(+E2)$ of the 563.9 keV transition and by the population via transitions from several 5^- levels [Fig. 8(g)].

The $K^\pi=5^-$ band at 870.00 keV. Besides the ground state band, Elze *et al.* [22] found by Coulomb excitation a new rotational band built on a level at ~870 keV. Since collective states are selectively populated by Coulomb excitation, this band was interpreted as the γ vibration with $K^\pi=5^-$ associated with the ground state configuration. In agreement with these data, a 5^- bandhead can be assigned, which decays to the ground state by an $E2$ transition and by a weak transition to the 6^- bandhead at 563.9 keV [Fig. 8(g)]. We note that there is an ambiguity with respect to the ARC data in this energy range. The two 5^- states at 868.1 and 870.0 keV correspond to the energy and intensity of the ARC line at 868.9 keV. However, the 4^+ state at 871.3 keV, which is discussed in Sec. VII, is not accounted for by the ARC results. The 6^- member of this band was placed near 1002 keV [22]; it is weakly populated by neutron capture and can be assigned at 1000.84 keV. However, this assignment is less well established, since the ground state transition is obscured by a ^{177}Lu line.

VI. COUPLING OF GROUND STATE AND ISOMER

The energy levels discussed so far represent the basis for the identification of levels, which can decay to both the ground state *and* the isomer. For the unambiguous assignment of the corresponding gamma transitions it is mandatory to define the isomer energy as precisely as possible. This value has already been used for the energies given in Table I, but will be discussed in detail in this section. To this end, the results from the experiments at Grenoble are supplemented with data from the (d,p) measurement.

A. The isomer energy from the ^{175}Lu$(d,p)^{176}$Lu experiment

The (d,p) spectrum at low energies: the position of the isomer. At low excitation energies, the 7^- ground state band as well as the bands with $K^\pi=0^-$, 1^+, and 1^- are weakly populated in the (d,p) reaction. Figure 9 presents the corresponding spectrum that was calibrated via 5 well-established lines [34]. By this calibration, the distance of two levels is well defined, whereas the offset remains as a free parameter. The distance between the 8^- member of the ground state band and the isomer can be determined to $\Delta E=61.0\pm0.5$ keV. On the other

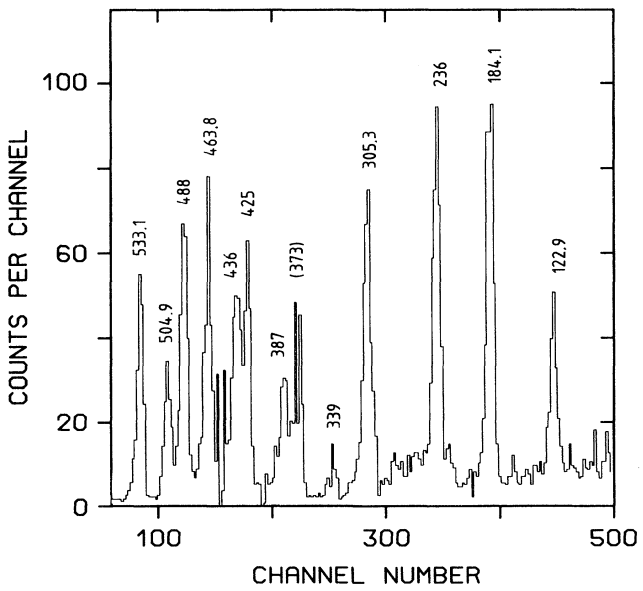

FIG. 9. The ^{175}Lu$(d,p)^{176}$Lu spectrum in the region of low energy levels (energies are in keV).

hand, the energy of the 8^- state is known from the Coulomb excitation studies [21] that was confirmed by this work to be $E=184.1$ keV. This yields the isomer energy to

$$E=123.1\pm0.5 \text{ keV} .$$

The (d,p) spectrum at higher excitation. The strongest lines in the spectrum of Fig. 10 are due to members of the rotational bands with the configuration $p\frac{7}{2}^+[404]$, $n\frac{1}{2}^-[510]$ and $K^\pi=3^-$ and 4^- [16,17]. Of these, the levels at 658.45, 751.89, 868.10, and 788.22 keV with $I^\pi=3^-$, 4^-, 5^-, and 4^-, respectively, are all well established. However, it was impossible to achieve a consistent energy calibration for all four levels, the line at 868.10 keV being significantly discrepant. A comparison of the measured intensity with the intensity pattern of Struble and Sheline [17] for the $K^\pi=3^-$ band yields an excess in the observed intensity. Therefore, this line is likely an unresolved doublet with a second contribution from the admixture of the $p\frac{7}{2}^+[404]+n\frac{3}{2}^-[512]$ configuration to the $K^\pi=5^-$ γ vibration at 870 keV; hence, it was not considered for the energy calibration. The energy scale based on the first three lines is in good agreement with the scale obtained for the low energy spectrum of the first run. It allows one to define the level energies of two states at 1030 and 1100 keV, which can be identified by means of the (n,γ) data as the 2^- and 3^- members of a new rotational band; in view of their relevance for the energy scale, these levels are described in detail below.

The $K^\pi=2^-$ band at 1029.695 keV; $p\frac{7}{2}^+[404]$-$n\frac{3}{2}^-[512]$. The bandhead is well defined by 7 gamma transitions [Fig. 8(d)] with $I^\pi=2^-$ according to the measured multipolarities. The 1030 keV line in the (d,p) spectrum can be associated with this level; the Nilsson configuration is suggested by its intense population in the transfer reaction, which leaves the ground state configuration of the odd proton unchanged. The $n\frac{3}{2}^-[512]$ state was also found to be significantly populated in the ^{174}Yb$(d,p)^{175}$Yb reaction [42].

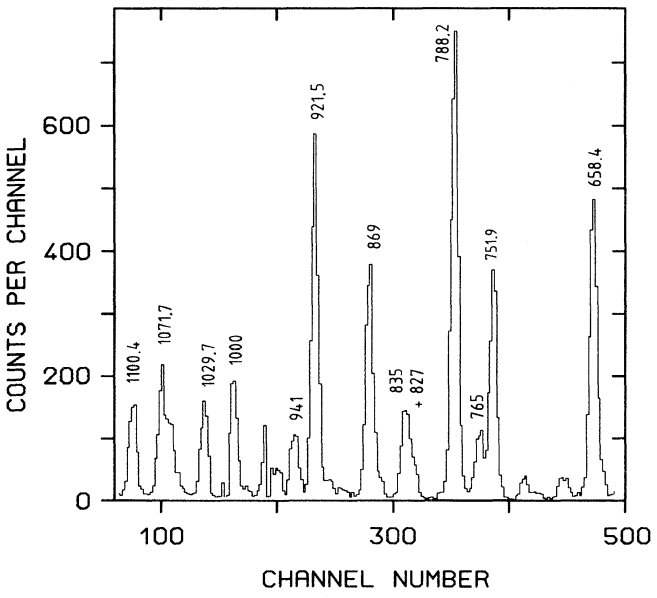

FIG. 10. The ^{175}Lu$(d,p)^{176}$Lu spectrum for levels at higher energies.

The 3^- member of this band is expected to lie 70 keV higher in excitation due to the theoretically estimated rotational parameter [26]. In this energy range, the ARC data [26] contain a level at 1100.6(3) keV with $I^\pi=3^-$ or 4^-, and a level at this energy is also observed in the (d,p) reaction. By the combination principle, these data yield a level at 1100.41 keV, which is depopulated by three transitions. Its additional confirmation as the 3^- member results from the $M1$ character of the 667.4 keV line.

The intraband transition to the 2^- bandhead is expected at an energy of 70.71 keV. Its intensity can be estimated from the depopulation of the bandhead to $(I_\gamma+I_e)/100n \leq 1$. This corresponds to a gamma intensity of $I_\gamma/100n \leq 0.09$ because of the large conversion coefficients for low energy transitions, and is just below the sensitivity limit of the crystal spectrometer in this energy range. Since the bandhead is more strongly depopulated by interband transitions than the 3^- member, there may be an undetected transition between these levels with an intensity $(I_\gamma+I_e)/100n \sim 0.5$.

Calibration of the (d,p) spectrum at high energies. With the two $K^\pi=2^-$ levels, the (d,p) spectrum could be calibrated without any extrapolation to higher energies. The energies in all three runs are consistent within uncertainties. Line energies measured in two runs were averaged, and the final values are given in Table III with uncertainties that include a systematic uncertainty of 0.2 keV resulting from the calibration.

B. Assignment of mediating transitions

The $K^\pi=4^-$ band at 788.219 keV; $p\frac{7}{2}^+[404]+n\frac{1}{2}^-[510]$. Minor *et al.* [16] assigned a very intense line in the (d,p) spectrum of Struble and Sheline [17] as the 5^- member of this 4^- band. The energy of that level is defined by the present (d,p) data as 921.7 ± 0.2 keV, and the assignment to the 4^- band is confirmed by the intensity systematics and by the rotational parameter. The bandhead corresponds to the most intense line in the spectrum, so that the 5^- state is also expected to be strongly populated [17]. There are only two suitable lines in the (d,p) spectrum, at 921 and 869 keV. However, the 869 keV line assigned by Struble and Sheline [17] via intensity arguments can now be excluded, since it would require a rotational parameter $A=8.1$ keV, too different from the well-defined $A=11.6$ keV for the $K^\pi=3^-$ band of the same Nilsson configuration with antiparallel spin coupling. Such a large difference is not likely for two bands with the same two-particle configuration. The assignment of the 921 keV line yields $A=13.3$ keV, closer to the value for the 3^- band.

So far, no transitions were assigned to that 921 keV level. The search for the $M1$ intraband transition to the 4^- bandhead yields no suitable gamma line with $I_\gamma/100n > 0.1$, even if the energy window is increased to a few keV. However, two *weak* transitions to the 4^-

bandhead and to the 4^- member of the $K=3$ band could be found by means of the combination principle [Fig. 8(e)]. The preference for the interband transition may be explained by strong Coriolis mixing ($\Delta K=1$) [16].

On the other hand, the intensities of the two transitions are too small to account for the population of that level, which can be estimated from the population of neighboring $I^\pi=5^-$ levels to $I_\gamma/100n\sim 1$. The only explanation for the corresponding depopulation seems to be gamma transitions to the level system coupled with the ground state.

A combination of a direct transition to the 7^- ground state and a transition to the 6^- bandhead at 563.9 keV can indeed be found, defining a level energy of 921.47 keV. If this energy is adopted for the 5^- state under discussion, the energy of the isomer is then fixed by a corresponding chain of gamma transitions to

$$E=122.859\pm 0.009 \text{ keV} ,$$

in good agreement with the 123.1 ± 0.5 keV from the (d,p) data. The branching to the ground state is strong enough to account for a total depopulation of $I_\gamma/100n=0.9$ of the 5^- state.

The $K^\pi=4^-$ band at 722.921 keV; $p\frac{1}{2}^+[411]+n\frac{7}{2}^-[514]$. The isomer energy can be confirmed by a second chain of gamma transitions. It connects isomer and ground state through a level at 838.65 keV that exhibits almost the same decay properties as the 921.47 keV level: a strong $E2$ transition to the ground state and a $M1$ transition to the 563.9 keV bandhead with $K^\pi=6^-$ [Fig. 8(f)]. This assignment is confirmed by the clear coincidence between the transitions with 563.9 and 274.7 keV. Spin and parity of the 838.6 keV level are determined by the observed multipolarities to $I^\pi=5^-$.

A weak ($M1$) transition to the 4^- bandhead at 722.9 keV can be assigned to this 5^- level. With the well-established gamma cascade from this bandhead to the isomer, one obtains an isomer energy $E=122.851\pm 0009$ keV, perfectly consistent with the enchainment via the 921 keV level.

That the 838.6 keV state is indeed the 5^- member of the 4^- band at 722.9 keV is further supported by the (t,α) spectrum of Dewberry *et al.* [20], where the 4^- bandhead corresponds to the strongest line. Therefore, the 5^- member also should be significantly populated in the (t,α) reaction. Dewberry *et al.* [20] assumed that level at 864 keV and suggested corresponding gamma transitions from Balodis *et al.* [19]; however, these gamma assignments are now disproved by this work.

The present assignment of the 838.6 keV level as the 5^- member of the above 4^- band is consistent with both the (t,α) measurement and the ARC data. A strong peak in the (t,α) spectrum at 840 keV can be interpreted as an unresolved doublet, consisting of a contribution from the 3^- bandhead at 843 keV and another one from the 5^- level. Dewberry *et al.* [20] considered only the 3^- part, but their resolution of 14 keV was not sufficient to recognize a second line only 5 keV apart. The unweighted average of the lines is at 841.1 keV, in fair agreement with their energy of 840 ± 2 keV. This picture is supported by the ARC measurement, where a doublet at 842.9 keV is reported [26] consisting of a 3^- or 4^- and of a 2^- or 5^- level.

In summary, two independent chains of gamma transitions were identified, which are related to both the ground state and to the isomer and which fit in a very consistent way to all existing data. The isomer energies deduced from the two chains agree well within their respective uncertainties of 9 eV, yielding a final average of

$$E=122.855\pm 0.006 \text{ keV} .$$

In this work, the energies of all levels related to the isomer refer to this value.

VII. ADDITIONAL LEVELS COUPLED TO THE ISOMER

The $K^\pi=3^-$ band at 843.422 keV; $p\frac{1}{2}^+[411]-n\frac{7}{2}^-[514]$. This bandhead is strongly populated in the (t,α) reaction. Dewberry *et al.* [20] identified lines at 840 ± 2, 945 ± 2, and 1075 ± 5 keV with the 3^-, 4^-, and 5^- members of this band and assigned gamma transitions from Balodis *et al.* [19] to this scheme. All assignments of these gamma transitions were found to be inconsistent with the present data. Instead, new combinations were derived that are compatible with the energies from the (t,α) reaction [Fig. 8(f)].

The 3^- bandhead at 843.422 keV is established by four $M1$ transitions. The strongest, with $E_\gamma=120.499$ keV, leads to the 4^- bandhead at 722.921 keV with the same Nilsson configuration, which then decays to the 3^- bandhead at 658.445 keV by a highly converted 64.474 keV transition. Since this low energy transition is difficult to detect in the coincidence spectra, the decay can be confirmed by the observed coincidence between the 120.5 keV line and the 225.4 keV transition from the decay of the lower 3^- bandhead.

The 4^- member is expected at 945 ± 2 keV according to the (t,α) spectrum. The ARC data [26] include a level at 944.9 ± 0.3 keV that is compatible with an assignment $I^\pi=4^-$. Even within a relatively large energy window, the corresponding 101.5(3) keV intraband transition to the bandhead could not be identified. Instead, the 222.106 keV $M1$ transition was found to the 4^- bandhead at 722.921 keV, which leaves the Nilsson configuration unchanged. This is further confirmed by a coincidence with the 225.4 keV line. In addition to the 222.1 keV line, two weak transitions to bandheads with $K^\pi=3^-$ and 6^- were found as well. The resulting level energy of 945.027 keV is in perfect agreement with Refs. [20] and [26].

The 5^- member is placed at 1068.992(5) keV by the combination of four weak transitions. This energy is in agreement with the (t,α) measurement [20], and a 5^- level is also consistent with the ARC data [26], which predict a doublet centered at 1068.1 keV. Though the 5^- level appears to be established, its assignment to this 3^- band seems questionable, since the decay systematics do not resemble those of 3^- and 4^- members.

The $K^\pi=2^+$ band at 866.364 keV. The energy of this bandhead is determined by a combination of nine transi-

tions [Fig. 8(h)]. Spin and parity can be limited to 1^+ or 2^+ due to the strongest transitions populating $K^\pi=1^+$ bands. Since there are also transitions to 1^- bands with, in particular, one to a 3^- member, the 2^+ assignment is unambiguously confirmed.

There are two possible Nilsson configurations for a 2^+ band in this energy range [26]: $p\frac{9}{2}^-[514]$-$n\frac{5}{2}^-[512]$ or $p\frac{5}{2}^+[402]$-$n\frac{9}{2}^+[624]$. The strongest $M1$ transitions lead to the $K^\pi=1^+$ band, for which the wave function is dominated by the configuration $p\frac{7}{2}^+[404]$-$n\frac{9}{2}^+[624]$. Since the transition to the other 1^+ bandhead exhibits only half the intensity—though it were favored by the higher energy difference—the situation is certainly better described by the second configuration

$$p\tfrac{5}{2}^+[402]\text{-}n\tfrac{9}{2}^+[624] .$$

A transition to the $p\frac{7}{2}^+[404]$-$n\frac{9}{2}^+[624]$ configuration leaves the particle state of the odd neutron unchanged. The weaker transitions to the other 1^+ band may be explained by configuration mixing of the two bands. The dominating $E1$ decay mode feeds almost exclusively the 1^- band with the configuration $p\frac{5}{2}^+[402]$-$n\frac{7}{2}^-[514]$; this supports the above configuration of the 2^+ band, since these transitions leave the odd proton state unchanged.

The 3^+ member of the 2^+ band is established at 930.761(10) keV by 11 gamma transitions [Fig. 8(h)]. These transitions feed the $(I+1)$ members of those bands, where the members with spin I are populated by the decay of the bandhead. From the well defined multipolarities one obtains $I^\pi=2^+$ or 3^+ for the 930.765 keV level. The weak $E2$ character of the 736.42 keV transition to the 1^+ level and the observed transition to a 4^- level indicate $I^\pi=3^+$. The ARC data suggest a 2^+ or 5^+ level at this energy [26], but the intensity of primary gamma transitions following neutron capture at 24 keV also permits a 3^+ assignment, so that there is no contradiction between the ARC data and the above assignment. The intraband transition to the 2^+ bandhead proceeds mainly via K-conversion electrons of ~ 1 keV and falls below the sensitivity limit of the gamma spectrometer.

The intensity systematics of the interband transitions from the 2^+ band is such that the strongest transitions from a level with spin I lead to the $(I-1)$ member of the $p\frac{7}{2}^+[404]$-$n\frac{9}{2}^-[624]$ band, and the second strongest to the spin I member of the $p\frac{9}{2}^-[514]$-$n\frac{7}{2}^-[514]$ band. With the rotational parameter $A=10.7$ keV from the distance of the 2^+ and 3^+ levels, one would expect the 4^+ member to lie at ~ 1016 keV. This energy can be determined to 1015.37 keV by the combination of two transitions, which correspond well to the described intensity pattern. The corresponding level at 1017.9 keV from the ARC data [26] is probably an unresolved doublet consisting of the 1015.37 keV band member and a 4^+ or 5^+ level at 1019.93 keV which is given in Fig. 8(l).

$K^\pi=3^+$, 4^+ levels with $p\frac{1}{2}^-[541],n\frac{7}{2}^-[514]$. For this configuration, only the $K^\pi=4^+$ bandhead was known from Balodis *et al.* [19]; it could be established by a combination of transitions to the 1^+ bands [Fig. 8(i)]. The two strongest transitions were confirmed by the coincidence chains

(i) [147.6 keV-188.3 keV] ,

and

[147.6 keV-115.1 keV-139.4 keV] ,

(ii) [335.8 keV-66.2 keV-38.7 keV-71.5 keV] ,

and

[335.8 keV-104.9 keV-71.5 keV] .

The level spin and parity $I^\pi=4^+$ are defined by the $M1$ character of the two lines.

For this level, a rather long half-life of 7.8 ± 0.5 ns was found (Sec. III E), thus confirming the previous assignment as a bandhead [36]. According to model calculations [26], the only possible configuration for a 4^+ bandhead in this energy range is $p\frac{1}{2}^-[541]+n\frac{7}{2}^-[514]$. This is confirmed by the observation that the neutron configuration is preserved for the strongest transitions.

A clear coincidence of a strong $M1$ transition with the 335.8 keV line from the decay of the 4^+ level suggests a level at 734.369(2) keV with $I^\pi=3^+$, 4^+, or 5^+; this is confirmed by the ARC data [26], which yield a 3^+ or 4^+ level at 733.6(3) keV. The energy difference is less than 2.5 times the statistical uncertainty and, therefore, is not significant. Model calculations of the Gallagher-Moszkowski splitting [43] between the bandheads of the configuration $p\frac{1}{2}^-[541],n\frac{7}{2}^-[514]$ yield the 3^+ bandhead with an energy ~ 82 keV higher than the 4^+ bandhead, compatible with the difference between the 734.369 keV level and the 4^+ bandhead. Since the 99.2 keV transition to the 4^+ level is the strongest decay channel, the 734.369 keV state can be identified as the 3^+ bandhead.

The long half-life of the 4^+ level and the decay of the 3^+ bandhead indicates a strong hindrance for transitions from these bands to the 1^+ bands. Therefore, strong intraband transitions are to be expected between the various members of these bands. In particular, the $I=K+1$ members should only decay by an $M1$ transition to the bandhead, so that these transitions cannot be found with the Ritz combination principle alone. Since no other low energy transitions than the 99.2 keV line were observed in coincidence with the 335 keV line, these intraband transitions fall below the sensitivity limit of the coincidence measurement; this result appears plausible if these transitions are highly converted. Therefore, the first members of these bands can only be suggested but not firmly established by combining the present measurements with model calculations.

The rotational parameter was calculated to $A=6.8$ keV [26]. The comparison of these calculations with experimental data for ^{176}Lu by Hoff *et al.* [26] showed a mean deviation of only ~ 1 keV. Hence, an energy of ~ 54.4 keV is expected for the first $4^+\rightarrow 3^+$ intraband transition of the 3^+ band. The measured gamma spectrum shows two highly converted $M1$ transitions close to that energy, which could not be attributed elsewhere in the level scheme via the combination principle. Their relatively high intensities $(I_\gamma+I_e)$ indicate transitions between levels of intermediate spin, because only these are

sufficiently populated.

Hence, the 4^+ member of the 3^+ band can be suggested at 786.266 keV with the assignment of the 51.896 keV transition being the $4^+ \rightarrow 3^+$ transition. This is supported by the fact that it is the only placement for the 4^+ level consistent with the ARC measurement [26]. In the relevant energy range, the ARC data do not contain a 4^+ level, but a $I^\pi = 2^-$, 5^- doublet contribution to the 4^- level at 788.2 keV. Such a 2^- or 5^- level was not found in the present work. Since the intensity is particularly enhanced in the 24 keV neutron captures, one may suggest alternatively a second level of positive parity. The sum of the reduced intensities from a 4^- and a 4^+ singlet is in good agreement with the experimental intensities of the 788.2 keV level.

From this suggestion for the 4^+ level one obtains a rotational parameter of $A_{\text{exp}} = 6.49$ keV, which yields an energy of ~ 64.9 keV for the $5^+ \rightarrow 4^+$ transition in this band. The assignment of a measured $M1$ transition with 64.970 keV yields the 5^+ level at 851.236 keV. This tentative scheme is supported by a weak transition to the 4^+ bandhead and by the population from a 4^+ level at 1015.37 keV.

The 5^+ member of the 4^+ band can be suggested by means of an $M1$ transition with 58.597 keV, which is the only measured line that corresponds to the expected energy difference and that is not yet assigned elsewhere in the level scheme. The resulting energy of the 5^+ member would be 693.804 keV. This energy corresponds to a doublet contribution in the ARC data [26] near 687.8 keV, which was interpreted as the superposition of a 2^- state and a 3^+ or 4^+ state. The spectrum taken with 24 keV neutrons, which is sensitive to positive parity levels, shows two lines with $E_{\gamma 1} = 5619.4 \pm 1.5$ keV and $E_{\gamma 2} = 5626.1 \pm 1.0$ keV. The excitation energy of the compound nucleus E_B can be determined in that case from the energy of the $I^\pi = 3^-$, $K = 0$ level and the corresponding gamma transition:

$$E_B = E_\gamma + E_{3^-} = 6311.9 \pm 0.3 \text{ keV} .$$

The two contributions of the resolved doublet in the $E_n = 24$ keV spectrum yield then the level energies

$$E_1 = E_B - E_{\gamma 1} = 692.5 \pm 1.5 \text{ keV}$$

and

$$E_2 = E_B - E_{\gamma 2} = 685.9 \pm 1.0 \text{ keV} .$$

Of these, E_1 is in good agreement with the proposed 5^+ level, while E_2 is the known energy of the 2^- level. The reduced intensities of the primary gamma transitions indicate a $(5^+, 2^-)$ doublet as well [34].

The configuration $p\frac{9}{2}^-[514] \pm n\frac{1}{2}^-[510]$. The 5^+ bandhead at 657.142 keV has already been suggested by Balodis *et al.* [19]; it is clearly confirmed by the present coincidence data for the 284.6 keV $M1$ transition, though some of the previously assigned gamma transitions do not agree with the improved energy systematics [Fig. 8(i)]. From this $M1$ transition to the 4^+ member of a 1^+ band follows: $I^\pi = 3^+$, 4^+, or 5^+, and the two weaker transitions to the 5^+ and 6^+ members of the same 1^+ band reduce these possibilities to $I^\pi = 5^+$. This assignment is supported by the absence of a stronger transition to a 3^+ level.

Hoff *et al.* [26] report a doublet at 658.1 keV in the ARC data, consistent with the assignment of a 3^- and a 5^+ level. Since the 3^- level at 658.445 keV is well established, the 5^+ level is confirmed by the ARC data as well.

According to model calculations [26], the low energy bandhead corresponds to the two-particle configuration $p\frac{9}{2}^-[514] + n\frac{1}{2}^-[510]$. This assignment is supported by the fact that the observed $M1$ transitions to the 1^+ band change the configuration of the odd neutron only, while the proton configuration remains unaffected. All other transitions to lower levels would change both configurations, resulting in a reduced transition probability. However, the observed transitions to the 1^+ band should also be strongly hindered by the K-selection rule. This led Balodis *et al.* [19] to propose the assignment of a 22 keV K-allowed transition to the 4^+ bandhead based on the measurement of Minor *et al.* [16]. The energy difference between the 5^+ and 4^+ levels can be exactly defined by the present data to $\Delta E = 21.935(3)$ keV, significantly smaller than the 22.11(2) keV given in Ref. [16]. Since the energies in the two data sets are generally in good agreement, the energy difference cannot be due to a systematic effect; therefore, this assignment was not adopted. In our crystal spectrometer measurements, a 22 keV transition is below the detection limit.

The $K^\pi = 4^+$ bandhead of the configuration $p\frac{9}{2}^-[514]$-$n\frac{1}{2}^-[510]$ is expected at a higher energy than the 5^+ bandhead discussed above [20]. A well-established level at 871.275 keV can be identified with this 4^+ bandhead [Fig. 8(i)]. The strongest transition with 214.1 keV directly populates the 5^+ bandhead at 657.1 keV. It shows up in coincidence with the 284.6 keV decay line of the 5^+ level as well as with the strongest transitions in the further cascade.

The 871.275 keV level is also confirmed by two transitions to the 3^+ and 4^+ bandheads discussed above. The measured multipolarities imply $I^\pi = 4^+$ or 5^+, but the low energy transition to the 3^+ bandhead indicates a preference for the 4^+ assignment, since the $M1$ transition rate is expected to be higher than that for $E2$ according to the behavior of similar transitions. Since the 214.1 keV transition to the 5^+ bandhead is the strongest decay channel, it is plausible to identify this level with the 4^+ bandhead of the same two particle configuration. In turn, its decay systematics confirms the 657 keV level as a 5^+ bandhead; if this level were just the 5^+ member of the 1^+ band with similar energy and decay systematics, strong transitions from the 4^+ level at 871 keV to other band members would have been expected as well.

The 3^- bandhead at 957.894 keV. This level is fixed by six $M1$ transitions [Fig. 8(j)]; the well-established multipolarities yield $I^\pi = 3^-$ or 4^-, and the less well-established $M1$ character of the 270.035 keV transition to a 2^- level suggests $I^\pi = 3^-$. The ARC measurement [26] predicts a multiplet of negative parity levels at a mean energy of 958.5(3) keV, consistent with a triplet of $I^\pi = 3^-$ or 4^- levels. The two other lines in the triplet correspond to the 3^- bandhead at 960.193 keV discussed

below and to a 4^- level at 957.75 keV that was assigned to a 0^- band. The mean energy of the three levels is 958.6 keV, in perfect agreement with the ARC data.

The strongest transitions from the 957.894 keV 3^- level lead to the $K^\pi=3^-,4^-$ bandheads with the structure $p\frac{7}{2}^+[404]\pm n\frac{1}{2}^+[510]$. The 3^- level can be assigned as a bandhead because of the low intensities of transitions to bands of low K. Nilsson configurations, which satisfy the condition that only an odd particle state is changed in the strongest transitions, are

$$p\tfrac{7}{2}^+[404]\text{-}n\tfrac{1}{2}^-[521] \quad \text{or} \quad p\tfrac{5}{2}^+[402]+n\tfrac{1}{2}^-[510] .$$

The weaker transitions can all be explained by configuration mixing in the respective final states and yield no additional information with respect to the two possible assignments.

The 4^- member of that rotational band was found at 1067.424 keV. It decays to the bandhead as well as to those bands, which are populated by transitions from the 3^- level. The ARC measurement [26] reports a 3^- or 4^- level at 1068.1(3) keV with a possible 2^-, 5^- doublet contribution. If the 5^- level at 1068.977 keV is accounted for, the spin and parity assignment of the 4^- level is consistent with the ARC data.

The 3^- bandhead at 960.193 keV. This level is established by six gamma transitions [Fig. 8(j)]. The strongest decay channel contains two $E1$ transitions to the 1^+ band, which is built on the 194.37 keV level. From the measured multipolarities one obtains $I^\pi=2^-$ or 3^-, but the absence of a transition to a 1^+ level and the observed low energy transition to a 4^- bandhead suggests $I^\pi=3^-$. The assignment as a bandhead is justified by the relatively long half-life of 0.7 ns (Sec. III E).

However, no safe assignment can be given for the predicted bandheads [26]. A possible configuration would be

$$p\tfrac{7}{2}^+[404]\text{-}n\tfrac{1}{2}^-[521] ,$$

which was also considered as a possibility for the 3^- band at 957.89 keV. The strongest gamma transitions would then correspond to a change of the configuration for the odd neutron from $\frac{1}{2}^-[521]$ to $\frac{9}{2}^+[624]$ that requires a mixing of the $p\frac{7}{2}^+[404]\text{-}n\frac{9}{2}^+[624]$ configuration to the 1^+ band. A second configuration

$$p\tfrac{1}{2}^+[660]\text{-}n\tfrac{7}{2}^-[514]$$

can be suggested due to the Nilsson diagram for protons [44]. The excitation energy of the $p\frac{1}{2}^+[660]$ state should be higher than that of the $p\frac{1}{2}^-[541]$ orbital and is, therefore, expected above $\sim$750 keV. This odd-proton configuration was not considered in the model calculations of Hoff *et al.* [26], since there are no experimental data in neighboring odd-even nuclei. For this second assignment, the $E1$ transitions correspond to a change of the odd proton from $p\frac{1}{2}^+[660]$ to $p\frac{7}{2}^+[404]$.

The 0^- band $p\frac{9}{2}^-[514]\text{-}n\frac{9}{2}^+[624]$. This band is established by its $I^\pi=2^-$, 3^-, 4^-, and 5^- members. All these levels are confirmed by combinations of secondary gamma transitions and are consistent with the ARC data (Table III). It should be noted that the 2^- level is interpreted as part of the ARC doublet, which—together with the second state at 834.8 keV—yields the correct sum intensity and mean energy. These levels are interpreted as a rotational band because of their consistent decay systematics [Fig. 8(k)]: each member with spin I decays to the corresponding $(I+1)$ and $(I-1)$ members of the $K=0$ band with the ground state configuration.

This could be interpreted as a γ vibration built on the $K=0$ band or as a two particle excitation of low K. The first possibility can be excluded due to the low observed rotational parameter. The comparison with model calculations shows that the 0^- band

$$p\tfrac{9}{2}^-[514]\text{-}n\tfrac{9}{2}^+[624]$$

is the only two particle configuration with low K in this energy range. Such a band is expected to exhibit a Newby shift of the even spin members relative to the odd spin members. A separate treatment of even and odd spin members results in rotational parameters of $A=8.95$ and 8.84 keV, respectively. Hence, the 1^- and 0^- members can be predicted to occur at $E_1=795.1$ keV and at $E_0=778.7$ keV. Searching for levels with the same decay pattern as observed for the higher spin members leads to a 1^- level at 796.641 keV, very close to the expected value. This level is well established by the decay systematics and by the measured multipolarities. For the 0^- member, only an $M1$ transition to the 1^- level at 122.855 keV is to be expected; the tentative assignment of a weak $(M1,E2)$ transition yields an energy of 780.185 keV, also close to the predicted energy.

The energy sequence of this band can better be described by the expression [19]

$$E_I=AI(I+1)+BI^2(I+1)^2 .$$

For members with odd spin $I=1,3,5$ one obtains

$$A_{I,\text{odd}}=8.607 \text{ keV} \quad \text{and} \quad B_{I,\text{odd}}=0.00547 \text{ keV} ,$$

and the corresponding values for members with even spin $I=0,2,4$ are

$$A_{I,\text{even}}=8.629 \text{ keV} \quad \text{and} \quad B_{I,\text{even}}=0.0125 \text{ keV} .$$

Since the 0^- level was included, the parameters for the even members are less well established; but from the small differences one may conclude, in turn, that the 0^- level was correctly assigned. The result of $A=8.6$ keV is in good agreement with the calculated value of 9.1 keV [26].

From the level sequence one obtains a Newby shift of $E_N=-0.39$ keV. This shift is much smaller than the theoretical estimate of $E_N=-30$ keV [43]. A discrepancy in the opposite direction is observed for the $K^\pi=0^-$, $p\frac{7}{2}^+[404]\text{-}n\frac{7}{2}^-[514]$ band, where the observed Newby shift is much larger than theoretically predicted.

The 4^+ bandhead at 985.569 keV. This level is fixed by three $M1$ transitions to bandheads with $K^\pi=3^+$, 4^+, and 5^+, so that spin and parity $I^\pi=4^+$ are unambiguously defined [Fig. 8(l)]. The assignment of the strongest $M1$ transitions is confirmed by the coincidences

350.4 keV-335.8 keV

and

251.2 keV-99.2 keV-335.8 keV .

The 251.2 keV line has to be interpreted as an unresolved doublet since the coincidence data as well as the energy combinations are also compatible with an additional assignment as a 1^- (637 keV)$\rightarrow 1^-$ (386 keV) transition. The intensity of the $4^+\rightarrow 3^+$ transition is, therefore, smaller than the measured intensity of the doublet. The decay systematics indicates a bandhead with $K^\pi=4^+$; the possible not yet assigned configurations from the model calculations of Hoff *et al.* [26] are

$$p\tfrac{1}{2}^+[411]\text{-}n\tfrac{9}{2}^+[624]$$

or

$$p\tfrac{9}{2}^-[514]\text{-}n\tfrac{1}{2}^-[521] .$$

For each of these assignments, the strongest observed transitions imply that *both* configurations are changed. This is compatible with the relatively long half-life of 1.2 ns (Sec. III E). Since the transition to the 5^+ bandhead is weaker than the transition to the 4^+ bandhead, it is likely that both particle configurations are changed in the first transition as well. This results in the assignment of the configuration

$$p\tfrac{1}{2}^+[411]\text{-}n\tfrac{9}{2}^+[624]$$

for the 4^+ bandhead at 985.569 keV. It is confirmed by a weak transition to the 3^- band at 843 keV, which has the same odd proton configuration.

Other levels in Figs. 8(e) to (m). A number of additional levels coupled to the isomer can be inferred by the Ritz principle in combination with the coincidence data and the ARC results. These levels are suggested by the present data, but cannot be firmly established or be assigned to a particular configuration. For example, the 2^+ level at 792 keV is defined by a number of transitions [Fig. 8(h)]. However, it is not clear whether it is a bandhead or the member of a 0^+ band. Another important level is the 1032.4 keV state [Fig. 8(l)]. Apart from the transitions to the isomer it exhibits a significant branching to the ground state. The existence of this mediating level, which may be considered as a 5^- bandhead, is supported by a strong line in the ARC spectrum, which can now be interpreted as a doublet (Table IV).

VIII. ADDITIONAL LEVELS COUPLED TO THE GROUND STATE

A. The $K^\pi=8^+$ bands

The configuration $p\frac{7}{2}^+[404]+n\frac{9}{2}^+[624]$. Previously, the 8^+ bandhead of this configuration was placed at 404 keV [19], but was not considered as firmly established. With the present data, this bandhead can now be unambiguously placed at 424.891 keV. The level decays by two gamma transitions to the ground state band, which both satisfy the energy combination principle and exhibit the correct multipolarity [Fig. 8(m)]. Furthermore, the 240.76 keV transition to the 8^- level is observed in coincidence with the 184.1 keV decay line of that level. The (d,p) spectrum contains a weak line at 425.2(3) keV that can be attributed to the 8^+ bandhead, since it does not correspond to any of the known levels related to the isomer. The fact that it is populated in (d,p) but not in (t,α) implies a $p\frac{7}{2}^+[404]$ structure of the bandhead, confirming the above assignment.

The 9^+ and 10^+ members of this band can also be inferred from the (d,p) data, but there are no corresponding gamma transitions, since these levels are too weakly populated in neutron capture. Up to $\sim$850 keV, only three lines could not be identified with levels from the (n,γ) data; if two of these are assigned as the 9^+ member at 615.2(2) keV and the 10^+ member at 826.4(2) of the 8^+ band, their distances imply a rotational parameter $A=10.57(1)$. This value is close to that for the 1^+ band ($A=10.96$ keV) of the same Nilsson configuration but with antiparallel spin coupling of the unpaired particles.

The configuration $p\frac{9}{2}^-[514]+n\frac{7}{2}^-[514]$. The 8^+ and 9^+ members of this band were attributed to the 486(3) keV and 683(3) keV lines in the (t,α) spectrum [20]. With the present (n,γ) data only a tentative assignment can be given for the decay of the 8^+ bandhead [Fig. 8(m)]. The 683 keV level can also be attributed to a weak line at 681.5(3) keV in the (d,p) spectrum. The population in both transfer reactions may be explained by configuration mixing with the other 8^+ band, similar to the situation found for the 1^+ bands. The (t,α) spectrum contains an unassigned line at 889(10) keV that corresponds to a weak line at 895.1(7) keV in the (d,p) spectrum. If these lines are attributed to the 10^+ member, the more precise energies from the (d,p) reaction yield $A=10.7(1)$ keV, consistent with the entire energy sequence; hence, this 895 keV level can indeed be considered as a member of this band [Fig. 8(m)].

B. The $K^\pi=7^+$ bandheads

Three bandheads with $K^\pi=7^+$ are predicted for the energy range $750<E<1000$ keV with the configurations

$$p\tfrac{5}{2}^+[402]+n\tfrac{9}{2}^+[624] ,$$

$$p\tfrac{9}{2}^-[514]+n\tfrac{5}{2}^-[512] ,$$

$$p\tfrac{7}{2}^+[404]+n\tfrac{7}{2}^+[633] .$$

All these levels could be identified on the basis of the present results.

The level at 734.033 keV. This level can be assigned as a 7^+ bandhead by the coincidence between the 240.8 keV decay line of the 8^+ bandhead and a 309.1 keV line; it is also consistent with the multipolarity and intensity of the 309.1 keV transition. The suggested Nilsson configuration is

$$p\tfrac{5}{2}^+[402]+n\tfrac{9}{2}^+[624] ,$$

which explains the transition to the 8^+ bandhead as a change $p\frac{5}{2}^+[402]\rightarrow p\frac{7}{2}^+[404]$, similar to the 1^- band at 386 keV. Transitions to the ground state band would require a change of the configurations for both odd particles and are, therefore, hindered.

TABLE IV. Comparison of the experimental band head energies and rotational parameters with model calculations of Hoff *et al.* [26].

Configuration	K^π	$E_{\text{expt.}}$ (keV)	$E_{\text{theor.}}$ (keV)	$\Delta E_{\text{theor.}}$ (keV)	$E_{\text{expt.}} - E_{\text{theor.}}$ (keV)	$E_{\text{G.M. exp.}}$ (keV)	$E_{\text{G.M. theor.}}$ (keV)	$\frac{\hbar^2}{2\Theta_{\text{expt.}}}$ (keV)	$\frac{\hbar^2}{2\Theta_{\text{theor.}}}$ (keV)
$p\frac{7}{2}^+[404]$	7^-	0	0		0			11,5	
$n\frac{7}{2}^-[514]$	0^-	237	210		+27	246	219	11,3	11,5
$p\frac{9}{2}^-[514]$	1^+	194	234		−40			10,2	
$n\frac{7}{2}^-[514]$	8^+	488	450	123	+38	219	141	10,7	10,7
$p\frac{7}{2}^+[404]$	1^+	339	278		+61			11,0	
$n\frac{9}{2}^+[624]$	8^+	425	452	27	−27	12	107	10,6	9,5
$p\frac{5}{2}^+[402]$	1^-	387	391		−4			11,8	
$n\frac{7}{2}^-[514]$	6^-	564	577	57	−13	120	130	11,5	11,3
$p\frac{7}{2}^+[404]$	1^-	638	575		+63			12,3	
$n\frac{5}{2}^-[512]$	6^-	766	736	66	+30	66	109		12,5
$p\frac{1}{2}^+[411]$	4^-	723	532		+191			11,6	
$n\frac{7}{2}^-[514]$	3^-	843	841	30	+2	128	321	12,7	11,8
$p\frac{7}{2}^+[404]$	3^-	658	590		+68			11,6	
$n\frac{1}{2}^-[510]$	4^-	788	710	37	+78	112	109	13,3	10,8
$p\frac{9}{2}^-[514]$	9^-	· · ·	598						
$n\frac{9}{2}^+[624]$	0^-	780	654	150	+126			8,6	9,1
$p\frac{1}{2}^-[541]$	4^+	635	676		−41			(5,8)	
$n\frac{7}{2}^-[514]$	3^+	734	758	215	−24	103	89	(6,5)	6,8
$p\frac{5}{2}^+[402]$	7^+	734	746		−12				
$n\frac{9}{2}^+[624]$	2^+	866	810	84	+56	186	112	10,7	9,6
$p\frac{7}{2}^+[404]$	4^-	(908)	792		+116				
$n\frac{1}{2}^-[521]$	3^-	960	906	181	+53	65	126	13,7	12,6
$p\frac{5}{2}^+[402]$	3^-	958	1001		−43				
$n\frac{1}{2}^+[510]$	2^-	· · ·	1105	94			115		10,8
$p\frac{9}{2}^-[514]$	5^+	657	852		−195				
$n\frac{1}{2}^-[510]$	4^+	871	992	160	−121	224	150		10,3
$p\frac{1}{2}^+[411]$	4^+	986	868		+118				
$n\frac{9}{2}^+[624]$	5^+	· · ·	1094	56			216		9,9
$p\frac{9}{2}^-[514]$	7^+	709	872		−163				
$n\frac{5}{2}^-[512]$	2^+	· · ·	982	189			160		11,7

TABLE IV. (*Continued*).

Configuration	K^π	$E_{\text{expt.}}$ (keV)	$E_{\text{theor.}}$ (keV)	$\Delta E_{\text{theor.}}$ (keV)	$E_{\text{expt.}}-E_{\text{theor.}}$ (keV)	$E_{\text{G.M. exp.}}$ (keV)	$E_{\text{G.M. theor.}}$ (keV)	$\frac{\hbar^2}{2\Theta_{\text{expt.}}}$ (keV)	$\frac{\hbar^2}{2\Theta_{\text{theor.}}}$ (keV)
$p\frac{7}{2}^+[404]$	0^+	. . .	877						
$n\frac{7}{2}^+[633]$	7^+	854	1020	132	−166		75		9,7
$p\frac{7}{2}^+[404]$	5^-	835	881		−46			11,5	
$n\frac{3}{2}^-[512]$	2^-	1030	927	3	+103	229	82	11,8	11,8
$p\frac{1}{2}^-[541]$	4^-	. . .	973	242			70		6,2
$n\frac{9}{2}^+[624]$	5^-	1032	1050						
$p\frac{5}{2}^+[402]$	5^-		1000	123			169		12,3
$n\frac{5}{2}^-[512]$	0^-	. . .	1117						
$p\frac{9}{2}^-[514]$	4^+	(1020)	1051	304	−31		130		11,9
$n\frac{1}{2}^-[521]$	5^+	. . .	1193						

The level at 854.67 keV. This level is derived from two transitions to the 7^- ground state and to the 8^+ bandhead. Spin and parity of the 854.67 keV level are $I^\pi=7^+$ or 8^+ according to the multipolarities of these transitions. For the assignment of this level as a bandhead, $K^\pi=7^+$ remains as the only possible two-particle state in this energy range. Both transitions occur to levels with the odd proton configuration $\frac{7}{2}^+[404]$, so that this configuration is also to be expected for the 7^+ bandhead; the decay changes only the odd neutron configuration, restricting the possible configurations for the 7^+ bandhead to

$$p\tfrac{7}{2}^+[404]+n\tfrac{7}{2}^+[633]\ .$$

The level at 709.23 keV. The 7^+ bandhead with the configuration

$$p\tfrac{9}{2}^-[514]+n\tfrac{5}{2}^-[512]$$

is placed at 709.23 keV by the combination of two transitions. The 221.4 keV $M1$ transition to the 8^+ bandhead at 487 keV indicates an odd proton configuration $p\frac{9}{2}^-[514]$ for that level. The 709 keV transition is part of a doublet that could not be completely resolved neither in the gamma nor in the conversion electron spectra. Therefore, the multipolarity of the transition could not be determined reliably in spite of its high intensity; a fit of the electron spectrum indicates an $E2$ transition, but an $E1$ character could also be possible if most of the intensity is due to the stronger $M1$ part of the doublet. In view of this uncertainty and of the weakly established gamma transition to the 8^+ bandhead, the 709.23 keV level cannot be firmly assigned at present.

C. The $K^\pi=6^-$ and 5^- bandheads

The $K^\pi=6^-$ band $p\frac{5}{2}^+[402]+n\frac{7}{2}^-[514]$. The well-established 6^- bandhead at 563.9 keV was discussed in Sec. V B. The 7^- member was suggested by Dewberry *et al.* [20] at 757(4) keV on the basis of the (t,α) spectrum. Their assignment of a 194.2 keV gamma line as the transition to the bandhead could, however, not be confirmed. Instead, this line was assigned to the 3^- level at 957.89 keV [Fig. 8(j)].

Lesko *et al.* [45] found in a recent coincidence measurement that the 6^- bandhead is fed by a 161.28 keV transition. The $M1$ character of that line, and the fact that there are no other transitions from the corresponding 725.2 keV level, support its assignment as the 7^- member [Fig. 8(g)]. In the (t,α) measurement [20], the resolution of $\sim$14 keV was not sufficient to distinguish this level from the strongly populated 4^- bandhead at 722.9 keV. The new assignment yields a rotational parameter $A=11.52$ keV, in good agreement with that for the 1^- band with the same Nilsson configuration ($A=11.76$ keV). This value implies the 8^- member to lie at 909.5 keV; possibly, a 909 keV line in the (t,α) spectrum corresponds to that state.

The $K^\pi=6^-$ band $p\frac{7}{2}^+[404]+n\frac{5}{2}^-[512]$. The combination of three gamma transitions defines a level at 765.68 keV [Fig. 8(g)]. The two $M1$ transitions to the 7^-

ground state and to the 6^- bandhead at 563.9 keV yield $I^\pi = 6^-$ or 7^-. A 7^- bandhead is not expected at this energy, and the 7^- member of the 6^- band at 563 keV can be assigned otherwise; therefore, this level is assigned as the 6^- bandhead of the above configuration. The transition to the neighboring 6^- bandhead is consistent with the decay systematics of the 1^- band of the same configuration, which also exhibits strong transitions to the neighboring 1^- band.

The (d,p) spectrum contains a line at 764.8 ± 1.1 keV. Though part of its intensity is definitely due to the 763.6 keV members of the $K = 1^-$ band, it is plausible to interpret this line as a doublet dominated by the 6^- bandhead, since the populations of all other members of the 1^- band are significantly weaker. The 7^- member of that band can be placed at 941.076 keV by the combination of a 941.5 keV line in the (d,p) spectrum with a suitable $M1$ transition to the bandhead. The resulting rotational parameter $A = 12.5$ keV is found to agree well with that for the 1^- band of the same configuration.

The $K^\pi = 5^-$ *band* $p\frac{7}{2}^+[404] + n\frac{3}{2}^-[512]$. The level at 834.809 keV is established by an $E2$ transition to the ground state and by an $M1$ transition to the 6^- bandhead at 563.9 keV [Fig. 8(g)]; these multipolarities imply $I^\pi = 5^-$.

A corresponding line of intermediate intensity and with the correct energy is observed in the (d,p) spectrum, and can be attributed to that level, indicating the ground state configuration for the odd proton. This means that a 5^- bandhead is characterized by the above Nilsson configuration. The comparison with the ^{174}Yb$(d,p)^{175}$Yb reaction [42] shows that the $n\frac{3}{2}^-[512]$ configuration is populated with average intensity. Therefore, this state should yield significant lines in the ^{175}Lu$(d,p)^{176}$Lu reaction as well.

The 6^- member was assigned at 972.519 keV, but is less well established. By itself, the suggested energy combination is not significant enough due to the relatively large uncertainties in gamma-ray energy, but the assignment is supported by the observation of a 971.6(7) keV line in the (d,p) spectrum. The rotational parameter of $A = 11.5$ keV would also be in good agreement with the theoretically expected value of 11.8 keV.

IX. INTENSITY BALANCE AND ISOMERIC RATIO

The population of assigned levels. In total, 270 measured gamma transitions could be placed in the present level scheme. Almost all of the remaining 239 gamma lines have either small intensities or are contaminated by transitions in ^{177}Lu and are, therefore, questionable. The important contribution of the conversion electron intensities was calculated for all transitions with known multipolarities. The total intensity of the measured electromagnetic transitions is then

$$\sum_{\text{meas}} (I_\gamma/100n + I_e/100n) = 349 \ .$$

Since the intensity of all assigned transitions is

$$\sum_{\text{assig}} (I_\gamma + I_e)/100n = 318 \ ,$$

more than 91% of the measured intensity is represented by the present level scheme.

Apart from energy systematics, the information from transition intensities is another important means for the experimental configuration of the proposed levels. In particular, the population of a correctly assigned level should never exceed its depopulation; this is verified for the respective experimental uncertainties in the population balance, which is given in Ref. [34].

The partial capture cross sections to ground state and isomer. These partial cross sections can be derived from the relative intensities of all electromagnetic transitions to either the ground state or to the isomer. Since 91% of the measured intensities could be assigned in the extended level scheme, this cross section ratio can be estimated via the population balance.

From the assigned transitions one obtains a fractional population of 11% for the ground state and of 89% for the isomer. The residual population from unknown levels at high energies can be estimated via the intensity balance [34]. Even levels with intermediate spin, which can be populated by primary gamma transitions, exhibit residual populations $I_\gamma/100n \leq 5$, whereas this value is below 1 or near 0 for levels with spins that are very different from the compound spins, e.g., for the 8^- member of the ground state band or the 0^- bandhead. A conservative estimate can, therefore, be obtained by assuming a residual population of $I_\gamma/100n \leq 5$ for the 7^- ground state and the 1^- isomer.

An upper limit for the partial cross section to the ground state results then from the extreme assumption that the residual population of the isomer can be neglected and that $I_\gamma/100n = 5$ for the ground state. Accordingly, the lower bound follows from the assumption that only the isomer is additionally fed from high energy levels. With the respective modifications of the intensity normalization one obtains for the isomeric ratio

$$0.848 < R = \sigma_p(i)/\sigma_{\text{tot}} < 0.895 \ ,$$

where $\sigma_p(i)$ and σ_{tot} are the partial and total capture section of ^{175}Lu.

The present measurements were performed in a perfect thermal spectrum and can, therefore, be compared to previous data. We note a significant discrepancy with respect to the thermal isomeric ratio of $R = 0.70 \pm 0.04$ quoted by Mughabghab [46], whereas the result of a recent measurement at higher energies ($R = 0.89 \pm 0.04$ around 25 keV, Ref. [47]) is in good agreement with the present value.

X. COMPARISON TO MODEL CALCULATIONS

The experimentally extended level scheme can be compared with the theoretical estimates of Hoff *et al.* [26], who used a semiempirical model for estimating the bandhead energies and rotational parameters for each rotational band. These calculations are based on (i) estimated excitation energies of the two odd particle configurations as deduced from the *experimental* data of neighboring nuclei, and (ii) *theoretically* determined values for the Gallagher-Moszkowski splitting and for the Newby terms

of $K=0$ bands [43] for consideration of the residual interaction between odd proton and odd neutron.

In general, the experimental excitation energies of odd particle states differ in neighboring odd-even nuclei. Therefore, Hoff *et al.* [26] used the respective mean values of two different neighbors, and adopted the deviation from the mean as an estimate for the uncertainties of their calculated bandhead energies. The effect of the calculated terms for the residual interaction are *not* considered in these uncertainties, ΔE_{theor}.

The present experimental results are listed in Table IV together with the calculated bandhead energies of Ref. [26]. Within this model, the differences between experimental and calculated values may be due either to the respective uncertainties of single-particle energies or to problems with the residual interaction. To make this point clear, the Gallagher-Moszkowski splittings (E_{GM}) are compared in Table IV as well. Deviations of the experimental bandhead energies beyond the range given by Hoff *et al.* [26] can normally be attributed to strong differences in E_{GM}.

For some bands, configuration mixing can be another reason for differences in the bandhead energies. One such example is the $K^{\pi}=4^{-}$ bandhead at 723 keV, which combines the configurations $p\frac{1}{2}^{+}[411]+n\frac{7}{2}^{-}[514]$ and $p\frac{7}{2}^{+}[404],n\frac{1}{2}^{-}[510]$. The latter admixture is experimentally justified by the population of this level in the (d,p) reaction. In this case, a relatively large difference in the bandhead energy of 191 keV is observed.

The mean deviation for all 29 known bandheads amounts to $\sim$70 keV, a satisfactory confirmation of the model calculations. The agreement between experiment and theory is even better for the rotational parameters. Parallel and antiparallel couplings of the odd particles are not distinguished by the model calculations, but the experimental results for the two couplings of a given Nilsson configuration exhibit only small differences. The mean deviation of all known rotational parameters from their calculated counterparts is 0.6 keV.

An important question for the astrophysical interpretation of the present data is how many of the theoretically expected levels were successfully identified. Comparison of experimental and calculated bandheads in Table IV shows that *all* theoretically predicted bandheads with spin $1\leq I\leq 8$ are experimentally confirmed; hence, one may conclude that the experimental level scheme in this spin range is now complete up to 950 keV.

At still higher energies, the level scheme starts to become incomplete. In this energy range, the model calculations are also incomplete, because there is not much experimental information from neighboring nuclei. In addition to single-particle excitations, collective phenomena such as core vibrations start to play a role around 1 MeV. This means that a vibrational state can be built on each two-particle configuration. The excitation energy is then approximately given by the sum of the two-particle and the vibrational energy. The lowest γ vibration being known at 870 keV implies that such states start, in any case, beyond $\sim$900 keV.

In summary, it can be stated that in the spin range $1\leq I\leq 8$ all expected energy levels in ^{176}Lu have been identified up to at least 900 keV. This holds in particular for *all* low energy levels that connect the ground state with the isomer. The mediating level with the lowest energy was identified as the $I^{\pi},K=5^{-}$, 4 state at 838.64 keV. The implications of these results for the stellar origin of ^{176}Lu and its astrophysical consequences will be discussed in the following paper.

ACKNOWLEDGMENTS

We thank O. W. B. Schult for helpful discussions concerning the (n,γ) experiments, and R. Smithey for the preparation of the samples for the (n,e^{-}) measurements. Two of us (W. A. and P. P.) are indebted for financial support to the ILL Grenoble and to the Bulgarian Ministry of Science and Education (Contract Nos. 257 and 258).

*Present address: Asea Brown Boveri, Corporate Research, CH-5405 Baden, Switzerland.

†Universität Tübingen, Physikalisches Institut, D-7400 Tübingen 1, Germany.

‡Universität Giessen, II. Physikalisches Institut, D-6300 Giessen, Germany.

[1] J. Audouze, W. A. Fowler, and D. N. Schramm, Nature **238**, 8 (1972).

[2] M. Arnould, Astron. Astrophys. **22**, 311 (1973).

[3] H. Beer and F. Käppeler, Phys. Rev. C **21**, 534 (1980).

[4] R. A. Ward, 1980 (private communication).

[5] H. Beer, F. Käppeler, K. Wisshak, and R. A. Ward, Astrophys. J. Suppl. **46**, 295 (1981).

[6] H. Beer, G. Walter, R. L. Macklin, and P. J. Patchett, Phys. Rev. C **30**, 464 (1984).

[7] A. Veres and I. Pavlicsek, Acta Phys. Acad. Sci. Hung. **28**, 419 (1970).

[8] E. B. Norman and S. Kellogg, Astrophys. J. **291**, 834 (1985).

[9] L. Lakosi, I. Pavlicsek, and A. Veres, in *Capture Gamma-Ray Spectroscopy 1987,* edited by K. Abrahams and P. Van Assche (Institute of Physics, Bristol, 1988), p. S745.

[10] D. G. Gardner, M. A. Gardner, and R. W. Hoff, in *Capture Gamma-Ray Spectroscopy 1987,* edited by K. Abrahams and P. Van Assche (Institute of Physics, Bristol, 1988), p. S315; J. Phys. G (Suppl.) **14**, S315 (1988).

[11] Y. Watanabe, T. Mukoyama, and S. Shimizu, Phys. Rev. C **23**, 695 (1981).

[12] F. Käppeler, in *Capture Gamma-Ray Spectroscopy 1987,* edited by K. Abrahams and P. Van Assche (The Institute of Physics, Bristol, 1988), p. S297; J. Phys. G (Suppl.) **14**, S297 (1988).

[13] S. G. Nilsson, Mat. Fys. Medd. Dan. Vid. Selsk. **29**, No. 16 (1955).

[14] C. J. Gallagher, Jr. and S. A. Moszkowski, Phys. Rev. **111**, 1282 (1958).

[15] N. D. Newby, Jr., Phys. Rev. **125**, 2053 (1962).

[16] M. M. Minor, R. K. Sheline, E. B. Shera, and E. T. Jurney, Phys. Rev. **187**, 1516 (1969).

[17] G. L. Struble and R. K. Sheline, Yad. Fiz. **5**, 1205 (1966) [Sov. J. Nucl. Phys. **5**, 862 (1966)].
[18] B. P. K. Maier, Z. Phys. **184**, 153 (1965).
[19] M. K. Balodis, J. J. Tambergs, K. J. Alksnis, P. T. Prokofjev, W. G. Vonach, H. K. Vonach, H. R. Koch, U. Gruber, B. P. K. Maier, and O. W. B. Schult, Nucl. Phys. **A194**, 305 (1972).
[20] R. A. Dewberry, R. K. Sheline, R. G. Lanier, L. G. Mann, and G. L. Struble, Phys. Rev. C **24**, 1628 (1981).
[21] M. Délèze, A. Bruder, S. Drissi, J. Kern, and G. L. Struble, Phys. Rev. C **36**, 1826 (1987).
[22] Th. Elze, private communication.
[23] G. Alaga, K. Alder, A. Bohr, and B. R. Mottelson, Mat. Fys. Medd. Dan. Vid. Selsk. **29**, No. 9 (1955).
[24] L. I. Rusinov, Usp. Fiz. Nauk **73**, 615 (1961) [Sov. Phys. Usp. **4**, 282 (1961)].
[25] K. E. G. Löbner, Phys. Lett. **26B**, 369 (1968).
[26] R. W. Hoff, R. F. Casten, M. Bergoffen, and D. D. Warner, Nucl. Phys. **A437**, 285 (1985).
[27] H. R. Koch, H. G. Börner, J. A. Pinston, W. F. Davidson, J. Faudou, R. Roussille, and O. W. B. Schult, Nucl. Instrum. Methods **175**, 401 (1980).
[28] H. G. Börner, J. Jolie, F. Hoyler, S. Robinson, M. S. Dewey, G. L. Greene, E. Kessler, and R. D. Deslattes, Phys. Lett. B **215**, 45 (1988).
[29] W. Mampe, K. Schreckenbach, P. Jeuch, B. P. K. Maier, F. Braumandl, J. Larysz, and T. von Egidy, Nucl. Instrum. Methods **154**, 129 (1978).
[30] F. Hoyler, H. G. Börner, S. Robinson, G. L. Greene, E. Kessler, and M. S. Dewey, J. Phys. G **14**, 161 (1988).
[31] J. A. Bearden, Rev. Mod. Phys. **39**, 78 (1967).
[32] G. Linker, private communication.
[33] T. von Egidy, Habilitation thesis, Technical University Munich (1968).
[34] N. Klay, Kernforschungszentrum Karlsruhe Report KfK-4675 1990.
[35] H. C. Pauli, U. Raff, and H. Bokemeyer, GSI Darmstadt Internal Report, 1988.
[36] W. Andrejtscheff, P. Manfrass, and W. Seidel, Nucl. Phys. **A226**, 142 (1974).
[37] W. Andrejtscheff, P. Petkov, Ch. Protochristow, L. K. Kostov, W. D. Hamilton, and F. Hoyler, J. Phys. G **12**, L151 (1986).
[38] M. Löffler, H. J. Scheerer, and H. K. Vonach, Nucl. Instrum. Methods **111**, 1 (1973).
[39] A. Chalupka, W. Berth, L. Schönauer, K. U. Bahnsen, J. Labedzki, H. J. Scheerer, H. K. Vonach, and G. Ziegler, Nucl. Instrum. Methods **217**, 113 (1983).
[40] R. C. Greenwood and R. E. Chrien, Nucl. Instrum. Methods **138**, 125 (1976).
[41] E. Browne, Nucl. Data Sheets **60**, 227 (1990).
[42] D. G. Burke, B. Zeidman, B. Elbek, B. Herskind, and M. Olesen, Mat. Fys. Dan. Vid. Selsk. **35**, No. 2 (1965).
[43] J. P. Boisson, R. Piepenbring, and W. Ogle, Phys. Rep. **26**, 99 (1976).
[44] C. M. Lederer and V. S. Shirley, *Table of Isotopes* (Wiley, New York, 1978).
[45] K. T. Lesko, E. B. Norman, R.-M. Larimer, B. Sur, R. M. Diamond, F. S. Stephens, M. A. Delaplanque, J. C. Bacelar, C. Beausang, and E. M. Beck, in Proceedings of the Fifth Workshop on Nuclear Astrophysics, edited by W. Hillebrandt and E. Müller (Max-Planck-Institut für Physik und Astrophysik Garching Report MPA/MP1 1989).
[46] S. F. Mughabghab, Neutron Cross Sections (Academic, Orlando, 1984), Vol. 1, Pt. B.
[47] W. R. Zhao and F. Käppeler, in *Astrophysical Ages and Dating Methods,* edited by J. Audouze, M. Cassé, and E. Vangioni-Flam (Editions Frontières, Gif sur Yvette, 1990), p. 357; Phys. Rev. C **44**, 506 (1991).